

Elsevier Editorial System(tm) for Geomorphology

Manuscript Draft

Manuscript Number: GEOMOR-445R2

Title: Landslide susceptibility assessment by bivariate methods at large scales: application to a complex mountainous environment

Article Type: Research Paper

Section/Category:

Keywords:

Corresponding Author: Mr. Yannick Thiery, PhD

Corresponding Author's Institution: UMR 6554 CNRS LETG-Geophen

First Author: Yannick Thiery, PhD

Order of Authors: Yannick Thiery, PhD; Jean-Philippe Malet, Researcher; Simone Sterlacchini, Researcher; Anne Puissant, Lecturer; Olivier Maquaire, Professor

Manuscript Region of Origin:

Abstract: Statistical assessment of landslide susceptibility has become a major topic of research in the last decade. Most progress has been accomplished on producing susceptibility maps at meso-scales (1:50,000-1:25,000). At 1:10,000 scale, which is the scale of production of most regulatory landslide hazard and risk maps in Europe, few tests on the performance of these methods have been performed. This paper presents a procedure to identify the best variables for landslide susceptibility assessment through a bivariate technique (weights of evidence, WOE) and discusses the best way to minimize conditional independence (CI) between the predictive variables. Indeed, violating CI can severely bias the simulated maps by over- or under-estimating landslide probabilities. The proposed strategy includes four steps: (i) identification of the best response variable (RV) to represent landslide events, (ii) identification of the best combination of

predictive variables (PVs) and neo-predictive variables (nPVs) to increase the performance of the statistical model, (iii) evaluation of the performance of the simulations by appropriate tests, and (iv) evaluation of the statistical model by expert judgment. The study site is the north-facing hillslope of the Barcelonnette Basin (France), affected by several types of landslides and characterized by a complex morphology. Results indicate that bivariate methods are powerful to assess landslide susceptibility at 1:10,000 scale. However, the method is limited from a geomorphological viewpoint when RVs and PVs are complex or poorly informative. It is demonstrated that expert knowledge has still to be introduced in statistical models to produce reliable landslide susceptibility maps.

1                   Landslide susceptibility assessment by bivariate  
2                   methods at large scales: application to a complex  
3                   mountainous environment.

4  
5                   Y. Thiery <sup>a\*</sup>, J.-P. Malet <sup>a</sup>, S. Sterlacchini <sup>b</sup>, A. Puissant <sup>c</sup>, O. Maquaire <sup>a</sup>

6  
7                   <sup>a</sup>UMR 6554 CNRS, LETG-Geophen, University of Caen-Basse Normandie, Esplanade de la Paix, BP 5183, F-  
8                   14032 Caen Cedex, France

9                   <sup>b</sup>National Research Council, Institute for the Dynamic of Environmental Processes, Piazza della Scienza, 1, I-  
10                  20126 Milano, Italy

11                  <sup>c</sup>UMR 2795 CNRS, IDEES-GeoSyscom, University of Caen-Basse Normandie, Esplanade de la Paix, F-14032  
12                  Caen Cedex, France

13

14

15                  **Abstract**

16                  Statistical assessment of landslide susceptibility has become a major topic of research in the last decade. Most  
17                  progress has been accomplished on producing susceptibility maps at meso-scales (1:50,000-1:25,000). At  
18                  1:10,000 scale, which is the scale of production of most regulatory landslide hazard and risk maps in Europe,  
19                  few tests on the performance of these methods have been performed. This paper presents a procedure to identify  
20                  the best variables for landslide susceptibility assessment through a bivariate technique (weights of evidence,  
21                  WOE) and discusses the best way to minimize conditional independence (CI) between the predictive variables.  
22                  Indeed, violating CI can severely bias the simulated maps by over- or under-estimating landslide probabilities.  
23                  The proposed strategy includes four steps: (i) identification of the best response variable (RV) to represent  
24                  landslide events, (ii) identification of the best combination of predictive variables (PVs) and neo-predictive  
25                  variables (nPVs) to increase the performance of the statistical model, (iii) evaluation of the performance of the

26 simulations by appropriate tests, and (iv) evaluation of the statistical model by expert judgment. The study site is  
27 the north-facing hillslope of the Barcelonnette Basin (France), affected by several types of landslides and  
28 characterized by a complex morphology. Results indicate that bivariate methods are powerful to assess landslide  
29 susceptibility at 1:10,000 scale. However, the method is limited from a geomorphological viewpoint when RVs  
30 and PVs are complex or poorly informative. It is demonstrated that expert knowledge has still to be introduced in  
31 statistical models to produce reliable landslide susceptibility maps.

32 *Keywords:* Landslide, Susceptibility assessment, GIS, Statistical modeling, Weights of evidence, Expert  
33 knowledge, French Alps

34

35

---

36 \* Corresponding author. Tel.: + 33(0)3 90 24 09 28  
37 E-mail address: thiery@equinoxe.u-strasbg.fr

38

39

## 40 **1. Introduction**

41 Assessing landslide hazard and risk with a minimum set of data, a reproducible methodology  
42 and GIS techniques, is a challenge for earth-scientists, government authorities and resource  
43 managers (Glade and Crozier, 2005). Landslide hazard assessment (LHA) estimates the  
44 probability of occurrence of landslides in a territory within a reference period (Varnes, 1984;  
45 Fell, 1994; van Westen et al., 2006). It is deduced from information on (i) landslide  
46 susceptibility expressed as the spatial correlation between predisposing terrain factors (slope,  
47 land use, superficial deposits, etc.) and the distribution of observed landslides in a territory  
48 (Brabb, 1984; Crozier and Glade, 2005) and, (ii) the temporal dimension of landslides related  
49 to the occurrence of triggering events (rainfalls, earthquakes, etc.). In most cases, landslide  
50 frequencies are difficult to obtain due to the absence of historical landslide records. Therefore,  
51 LHA is most of the time restricted to landslide susceptibility assessment (LSA) which is  
52 considered as a ‘relative hazard assessment’, and does not refer to the time dimension of  
53 landslides (Sorriso Valvo, 2002). Landslide susceptibility maps can be obtained by two

54 categories of methods: (i) direct approaches based on expert knowledge of the target area, and  
55 (ii) indirect approaches based on statistical algorithms.

56 The direct approaches are based on expert knowledge about the relation between the  
57 occurrences of landslides and their hypothesized predisposing factors. The approach  
58 necessitates the definition of expert rules leading to different susceptibility degrees (Soeters  
59 and van Westen, 1996). In France, the official methodology to assess landslide susceptibility  
60 and hazard is based on direct approaches. The methodology, called 'Plans de Prévention des  
61 Risques' (MATE/MATL, 1999) has been applied at 1:10,000 scale.

62 The main concept of the indirect approaches is that the controlling factors of future landslides  
63 are the same as those observed in the past (Carrara et al., 1995). Indirect approaches are based  
64 on statistical conditional analyses and on the comparisons of landslide inventories and  
65 predisposing terrain factors. The methods are applied at the scale of the terrain unit (TU)  
66 corresponding to a portion of hillslope possessing a set of predisposing factors, which differs  
67 from that of the adjacent units with definable boundaries (Hansen, 1984; Carrara et al., 1995).  
68 Indirect approaches predict landslide distribution (the response variable, RV) through a set of  
69 *a priori* independent terrain factors (the predictive variables, PVs).

70 Several bivariate (certainty factors and weights of evidence) or multivariate (logistic  
71 regression and discriminant analysis) approaches were developed for landslide susceptibility  
72 mapping. A synthesis of the available methods, their applicability and drawbacks, can be  
73 found in Yin and Yan (1988), Carrara et al. (1995), Chung et al. (1995), Soeters and  
74 van Westen (1996), Atkinson and Massari (1998), Aleotti and Chowdury (1999), Guzzetti et  
75 al. (1999), Clerici et al. (2002), Dai et al. (2002), van Westen (2004) and van Westen et al.  
76 (2006). In the scientific community it is commonly admitted that statistical analyses are more  
77 appropriate for susceptibility zoning at meso-scales (1:50,000 to 1:25,000) because of their

78 potential to minimize expert subjectivity (Soeters and van Westen, 1996; van Westen et al.,  
79 2006).

80 Although the bivariate approaches are considered as more robust and flexible (van Westen et  
81 al., 2003; Süzen and Doruyan, 2004), they present some limitations:

82 (i) The tendency to over-simplify the (input) thematic data (e.g. predisposing factors) that  
83 condition landslides, by taking only what can be relatively easily mapped or derived  
84 from a DTM (van Westen et al., 2003, 2006).

85 (ii) The large sensitivity to the quality and accuracy of the thematic data, e.g., imprecision  
86 and incompleteness of landslide information, and limited spatial accuracy of information  
87 on the predisposing factors (Guzzetti et al., 2006). Application of the methods is  
88 relatively limited at large scales because most of thematic data are available only at  
89 meso-scales (1:50,000 to 1:25,000). Especially for most mountain areas a discrepancy  
90 remains between the scale of available data and the scale of landslide occurrence. For  
91 instance, geological maps and land-use maps are available only at scales from 1:50,000  
92 to 1:25,000 for most parts of the French Territory; also, only digital terrain models with  
93 a planimetric resolution of 50 m and a vertical accuracy of 2 to 3 m are available. These  
94 input data are not adapted to the analysis of landslide susceptibility at 1:10,000 scale  
95 (Thiery et al., 2003, 2004).

96 (iii) The singularity of predisposing factors for each landslide type, which forces us to  
97 analyse them individually in order to have distinct susceptibility maps (Atkinson and  
98 Massari, 1998; Kojima et al., 2000; van Westen et al., 2006).

99 (iv) The number of landslide events to incorporate in the statistical model in relation to the  
100 size of the study area (Bonham-Carter, 1994; Begueria and Lorente, 1999; van den  
101 Eeckaut et al., 2006).

102 (v) The use of statistically independent predictive variables in the application of bivariate  
103 methods. When the influence of a combination of predictive variables on the response  
104 variable is evident, the weight associated to each thematic factor is calculated  
105 independently and combined in a unique equation (Agterberg et al., 1993; Bonham-  
106 Carter, 1994). The probabilities computed with this equation may be different from  
107 those calculated directly from the input data. Therefore, applying the method requires to  
108 assume conditional independence (CI) of the dataset (Bonham-Carter et al., 1989;  
109 Agterberg et al., 1993; van Westen, 1993; Agterberg and Cheng, 2002; Thiart et al.,  
110 2003).

111 (vi) The absence of expert opinions if the method is applied by GIS experts and not by earth-  
112 scientist. In other words, the model should give satisfactory results in term of degree of  
113 fit, but should also correspond to the 'real world' (van Westen et al., 2003, 2006).

114 Some procedures were proposed to overcome these limitations and increase the robustness of  
115 landslide susceptibility assessments with indirect approaches through: (i) proper validation  
116 and reduction of simulation uncertainty (Chung and Fabbri, 2003; Chung, 2006; Guzzetti et  
117 al., 2006; van den Eeckaut et al., 2006), (ii) reduction of the costs of data acquisition (Greco  
118 et al., 2007), and (iii) introduction of expert knowledge to the statistical models used (van  
119 Westen et al., 2003).

120 Hence, the aim of this work is to ascertain a reproducible procedure to estimate landslide  
121 susceptibility with a bivariate approach at 1:10,000 scale in a complex mountainous  
122 environment, while limiting the collection of landslide and thematic data. The procedure  
123 adopted for this research includes four steps:

124 (i) Identification of the best way to calculate landslide probabilities based on the  
125 characteristics of the landslide inventory.

- 126 (ii) Identification of the most relevant combination of predisposing terrain factors avoiding  
127 conditional dependence.
- 128 (iii) Evaluation of the degree of model fit by statistical tests and comparisons with the  
129 landslide inventory.
- 130 (iv) Evaluation of the best indirect susceptibility map in comparison with a direct  
131 susceptibility map.
- 132 The procedure was applied to the north-facing hillslope of the Barcelonnette Basin (South  
133 French Alps) affected by several landslide types (Maquaire et al., 2003; Thierry et al., 2005;  
134 Malet et al., 2005).

135

## 136 **2. Geomorphological settings**

### 137 *2.1. Geomorphology of the Barcelonnette Basin*

138 The Barcelonnette Basin is representative of climatic, lithological, geomorphological and  
139 land-use conditions observed in the South French Alps, and is highly affected by landslide  
140 hazards (Flageollet et al., 1999). It is situated in the dry intra-Alpine zone, characterized by a  
141 mountain climate with a Mediterranean influence. Highly variable rainfall amounts (400 to  
142 1300 mm yr<sup>-1</sup>) occur with intense storms during summer and autumn. However, as pointed  
143 out by Flageollet et al. (1999), landslides there are not controlled only by climatic conditions;  
144 slope instability can occur after relatively dry periods whether or not preceded by heavy  
145 rainfalls.

146 The test site extends over an area of about 100 km<sup>2</sup>. Located on the north-facing hillslope  
147 (Fig. 1), it is characterized by a large variety of active landslides and is representative of the  
148 environmental conditions observed in the Barcelonnette Basin. The Ubaye River depicts the  
149 northern boundary, while the Sauze torrent delimits the western boundary; the southern and

150 eastern boundaries are represented by high crests of limestones and sandstones. The test site  
151 can be subdivided into two geomorphological units separated by a major fault in a north/south  
152 direction. The eastern unit is dominated by allochthonous sandstones outcrops, while the  
153 western unit is composed of autochthonous Callovo-Oxfordian marls (BRGM, 1974;  
154 Flageollet et al., 1999; Maquaire et al., 2003).

155 The eastern unit (ca. 40 km<sup>2</sup>) is drained by the Abriès torrent which cuts an asymmetric valley  
156 in highly fractured sandstones. The gentle slopes there (10-30°) are covered by moraine  
157 deposits of 2 to 15 m thick and by coniferous forests or grasslands (Fig. 2); these slopes are  
158 affected by shallow rotational or translational slides triggered by the undercutting of torrents.  
159 In contrast, the steep slopes (30-70°) are characterized by bare soils and affected by rockfalls  
160 on sandstones.

161 The western unit (ca. 60 km<sup>2</sup>), drained by four main torrents, presents an irregular topography  
162 of alternating steep convex slopes, planar slopes and hummocky slopes. The steepest convex  
163 slopes (>35°) are carved in black marl outcrops, and are very commonly gullied into badlands,  
164 or affected by rock-block or complex slides (Malet et al., 2005). The planar slopes (5-30°)  
165 composed of thick moraine deposits (from 6 to 20 m), are very often cultivated and affected  
166 by rotational or translational slides. The hummocky slopes are generally covered by forests  
167 and/or natural grasslands (Fig. 2), and affected by large relict landslides and/or surficial soil  
168 creep. Most landslides within the western unit are located along streams or on gentle slopes,  
169 where the contact of moraine deposits and black marls creates a hydrological discontinuity  
170 favourable for slope movements.

171

172 2.2. *Landslide data*

173 A landslide inventory was compiled at 1:10,000 scale through air photo-interpretation, field  
174 surveys and analysis of literature in years 2002 and 2003 by a geomorphologist (Thierry et al.,  
175 2003, 2004). Air-photo interpretation was carried out on 1:25,000-scale photographs (year  
176 2000) issued from the French Geographical Institute. Fieldwork was carried out between July  
177 2002 and July 2003 to complete the photo-interpretation. To reduce uncertainty linked to an  
178 expert in charge of mapping (Ardizzone et al., 2002; Wills and Mc Crinck, 2002), two  
179 degrees of confidence were defined for the photo-interpretation and information of available  
180 literature (landslide recognition or not), while three degrees of confidence (high, medium and  
181 low) were distinguished for the field survey. A mapping confidence index (MCI) in three  
182 classes (high, medium and low) was derived. Three hundred fourteen landslides were  
183 recognized, with 66% classified with a high MCI , 27% with a medium MCI and 7% with a  
184 low MCI. Among the 207 landslides with a high MCI, 10% are considered as relict, 8% are  
185 considered as latent, and 82% are considered as active. The active landslides can be grouped  
186 in three types (Table 1) according to the typology of Dikau et al. (1996).

187 Figs. 3 and 4 present the morphology and morphometric/environmental characteristics of the  
188 landslides. Shallow translational slides are relatively small and mainly located on steep slopes  
189 along streams. They occur on the weathered bedrock or in moraine deposits. Rotational slides  
190 are located along streams but more on gentle slopes than the shallow translational slides. They  
191 occur principally in moraine deposits or at the contact with the bedrock. Translational slides  
192 are located more on gentle slopes at the contact with the bedrock, and their sizes are very  
193 variable (Table 1).

194 The boundaries of active landslides were classified into two zones and digitized: (i) the  
195 landslide triggering zone (LTZ) and (ii) the landslide accumulation zone (LAZ, Fig. 3). The  
196 geometrical (perimeter, area, and maximal length) and geomorphological characteristics  
197 (typology and state of activity) were stored in a GIS database.

198 As the aim of this study is to locate areas prone to failures, only the LTZ of active landslides  
199 were introduced in the analysis (Atkinson and Massari, 1998; van den Eeckhaut et al., 2006).  
200 In statistical models, the total area of landslides (van Westen et al., 2003) or only the  
201 triggering area can be used to compute probabilities of landsliding (Chung and Fabbri, 2003;  
202 Remondo et al., 2003). According to the characteristics of the landslides, especially their run-  
203 out distances, a severe bias can occur when the landslide accumulation zone is taken into  
204 account in the model. Indeed, several classes of input data may be included in the probability  
205 calculation process, while in reality they were not the most important controlling factors.  
206 Therefore, Atkinson and Massari (1998), Sterlacchini et al. (2004), and van den Eeckhaut et  
207 al. (2006) proposed to use only one cell at the centre of the triggering zone. This procedure  
208 offers some advantages because it does not take into account the landslide boundaries and it  
209 does not attribute a too large influence to the largest landslides which exhibit more diversity  
210 in predisposing factors. However, if the results based on one cell at the centre of the triggering  
211 zone can be satisfactory, the final probabilities are not necessarily representative of the  
212 predisposing conditions at the onset of the landslide. Defining the most appropriate part of the  
213 landslide to compute the probabilities is therefore a prerequisite to understand how it  
214 influences the model results.

215

### 216 2.3. *Landslide predisposing factors*

217 The statistical analysis of the landslide inventory has outlined the main predisposing factors  
218 (predictive variable) to introduce in the statistical model. The thematic data (Table 2) are  
219 derived from (i) available national databases, (ii) air-photo interpretation analyses, (iii)  
220 satellite imagery analyses, and (iv) field surveys. The DTM (10-m resolution) was constructed  
221 by the kriging interpolation applied to a network of triplets, obtained from the digitisation of

222 contour lines in 1:25,000-scale topographic maps which were enlarged by the French  
223 Geographical Institute into 1:10,000 scale. Its accuracy is of about  $\pm 1$  m for the horizontal  
224 component, and  $\pm 2$  to 10 m for the vertical component, depending on relief.

225 The slope gradient map and the slope curvature map were derived from the DTM. The  
226 lithological map is based on the main lithological units described in a geological map  
227 produced by the French Geological Survey (BRGM, 1974) at 1:50,000 scale, and was  
228 completed by fieldwork. The surficial formation map was obtained by the segmentation of the  
229 landscape into homogeneous macro-areas closely associated with sediment facies (van  
230 Westen, 1993). The surficial formation thickness map was derived from direct observations of  
231 outcrops along streams and steep slopes. The land-use map was produced by the analysis of a  
232 Landsat ETM+ image (year 2000) fused with a SPOT-P image (year 1994); the boundaries of  
233 homogeneous land-use units were corrected by air-photo interpretation.

234

#### 235 2.4. *Direct landslide susceptibility map*

236 The direct landslide susceptibility map was elaborated with the French legal procedure for  
237 landslide hazard and risk at 1:10,000 scale (MATE/MATL, 1999; Leroi, 2005). This  
238 methodology requires a global overview of the area to identify sectors with homogeneous  
239 environmental characteristics for each landslide type. The methodology advises us to take into  
240 account the possibilities of landslide development for the forthcoming one hundred years.  
241 Four degrees of susceptibility were defined. The expert rules used to define the direct  
242 susceptibility classes are detailed in Table 3.

243

### 244 3. **Methodology and strategy**

245 3.1. *Weights-of-evidence (WOE): background*

246 3.1.1. *WOE method*

247 Weights-of-evidence (WOE) is a quantitative ‘data-driven’ method used to combine datasets.  
248 The method, first applied in medicine (Spiegelhater and Kill-Jones, 1984) and geology  
249 (Bonham-Carter, 1994), uses the log-linear form of the Bayesian probability model to  
250 estimate the relative importance of evidence by statistical means. This method was first  
251 applied to the identification of mineral potential (Bonham-Carter et al., 1990) and then to  
252 landslide susceptibility mapping (van Westen, 1993; van Westen et al., 2003; Süzen and  
253 Doruyan, 2004).

254 Prior probabilities (PriorP) and posterior probabilities (PostP) are the most important concepts  
255 in the Bayesian approach. PriorP is the probability that a TU (terrain unit) contains the RV  
256 (response variable) before taking PVs (predictive variables) into account, and its estimation is  
257 based on the RV density for the study area. This initial estimate can be modified by the  
258 introduction of other evidences. PostP is then estimated according to the RV density for each  
259 class of the PV. The model is based on the calculation of positive  $W^+$  and negative  $W^-$   
260 weights, whose magnitude depends on the observed association between the RV and the PV.

261 
$$W^+ = \ln \frac{P(B | RV)}{P(B | \bar{RV})} \quad (1)$$

262 
$$W^- = \ln \frac{P(\bar{B} | RV)}{P(\bar{B} | \bar{RV})} \quad (2)$$

263 In Eqs. (1) and (2), B is a class of the PV and the overbar sign ‘ $\bar{\phantom{B}}$ ’ represents the absence of  
264 the class and/or RV. The ratio of the probability of RV presence to that of RV absence is  
265 called odds (Bonham-Carter, 1994). The WOE for all PVs is combined using the natural  
266 logarithm of the odds (logit), in order to estimate the conditional probability of landslide  
267 occurrence. When several PVs are combined, areas with high or low weights correspond to  
268 high or low probabilities of presence of the RV.

269

### 270 3.1.2. Hypothesis of the WOE method

271 As mentioned by Bonham-Carter (1994), the results of the WOE method are strongly  
272 dependent on the number of events introduced in the model (e.g. on the estimation of  
273 probabilities) and on the quality of the landslide inventory map. Therefore, probabilities are  
274 very low if the area is characterized by rare events, and the results have to be interpreted  
275 cautiously. Nevertheless, if the study area is covered by reasonable samples of events, the  
276 estimated weights can be stable and realistic.

277 The WOE method requires the assumption that input maps are conditionally independent. To  
278 meet this need, many statistical tests may be used (e.g.,  $\chi^2$ -test, omnibus test, and new  
279 omnibus test). A detailed review of the performance of these tests can be found in Agterberg  
280 and Cheng (2002) and Thiart et al. (2003). In case of violation of conditional independence,  
281 PVs which are dependent can be combined into a neo-variable (nPv) which is then used in  
282 the WOE method (Thiart et al., 2003). The weighted-logistic-regression method (WLR) may  
283 also be used to bypass the violation of conditional independence. However, if the density of  
284 the RV is low, this method severely underestimates PostP, and a number of the RV smaller  
285 than the observed value can be predicted (Thiart et al., 2003). Consequently, specific

286 procedures have to be used on large areas characterized by a low density of the RV (Begueria  
287 and Lorente, 1999; van den Eeckhaut et al., 2006).

288

### 289 3.2. *Employed methodology*

290 The employed methodology uses the main steps described by van Westen et al. (2003) and  
291 Guzzetti et al. (2006), i.e.: (i) aptitude of thematic data to construct a model, (ii) evaluation of  
292 the uncertainty level of probabilities, (iii) determination of the degree of model fit  
293 (performance) to an indirect landslide susceptibility map, and (iv) evaluation of the indirect  
294 landslide susceptibility map in comparison with a direct susceptibility map.

295 The first three steps were tested on a ‘sampling area’ of the study site (north-facing hillslope  
296 of the Barcelonnette Basin) characterized by the occurrence of the three types of landslides  
297 (Fig. 1). This test area extends over about 11 km<sup>2</sup> and is representative of the western and  
298 eastern terrain units described previously. The upper parts of the hillslopes were not included  
299 in the ‘sampling area’ because the environmental conditions are not representative of the  
300 landslides introduced in the analysis.

301 The probabilities of future landslide occurrence are calculated for each landslide type (only  
302 LTZs are introduced in the analysis) and a susceptibility map is created after the classification  
303 of PostP. Susceptibility classes were compared to the observed LTZs in the ‘sampling area’. If  
304 results were satisfactory, the statistical model was applied to the whole area with the same  
305 procedure (Fig. 5). Then, the final indirect landslide susceptibility map was assessed with the  
306 direct landslide susceptibility map with a confusing matrix and several statistical accuracy  
307 tests. Thus, a careful confrontation with a reference map was performed at each step. The  
308 statistical model was implemented in ArcView 3.2® through the ArcSDM extension (Kemp  
309 et al., 2001), and the size of the calculation cell was 10 m.

310

311 3.2.1. *Identification of the response variable (RV)*

312 Bayesian models are very sensitive to the number and quality of the RV. Over large areas  
313 characterized by complex thematic data, it can be very difficult to identify LTZs with high  
314 confidence. To deal with these limitations, the first two steps of the procedure are: (i) to  
315 identify the minimum number of cells representing the variability of the predisposing factors  
316 within LTZs, and (ii) to identify the best spatial location of cells to represent the variability of  
317 the predisposing factors within LTZs. For each landslide type, the same number of cells was  
318 introduced at each calibration phase. The initial number of cells in the LTZs examined in this  
319 study is 460.

320 The minimal number of cells to introduce in the model was estimated by a random sampling  
321 (10 to 100%) of the LTZ cells of each landslide type. The best spatial location of cells was  
322 estimated by selecting several cells' locations within the LTZs (Table 4). The computations  
323 were performed with a set of four *a priori* 'constant' thematic maps of PVs (slope gradient,  
324 surficial deposits, lithology, and land use). A landslide susceptibility map was then produced  
325 for each combination. The PostP distribution was analysed by expert judgment to define  
326 susceptibility classes. In former studies, the number of classes varied from two (e.g. stable  
327 and unstable; Begueria and Lorente, 1999) to six (null, very low, low, moderate, high, and  
328 very high susceptibility; Chacón et al., 2006). In this study, landslide susceptibility was  
329 classified into four (null, low, moderate, and high) for comparison to the direct landslide  
330 susceptibility map with the four classes. The relative error  $\xi$  was computed to evaluate the  
331 performance of the simulations:

332 
$$\xi = \frac{O_L - P_L}{O_L} \quad (3)$$

333 where  $O_L$  is the number of the observed landslide cells representing the LTZ of active  
334 landslides, and  $P_L$  is the number of the predicted landslide cells with the high susceptibility  
335 class. If the relative error decreases with the introduction of a RV, this RV is retained for the  
336 next simulation step (Fig. 5).

337

### 338 3.2.2. Identification of the predictive variables (PVs)

339 The performance of the PVs introduced successively in the statistical model was evaluated in  
340 terms of CI violation and distribution of PostP for each landslide type. Computations were  
341 performed with the best RV dataset identified previously. The procedure is as follows:

- 342 (i) Selection of the best PV dataset by expert judgement which takes into account the  
343 predisposing factors and classes associated with each landslide type;
- 344 (ii) Analysis of CI violation between each PV and the RV. As the  $\chi^2$ -test is very sensitive to  
345 the density of the RV introduced in the model (Thiart et al., 2003) and may increase the  
346 measure of the dependence between two PVs by 25 to 30% (Pistocchi et al., 2002;  
347 Dumolard et al., 2003), the Cramer's  $V$  coefficient (Kendall and Stuart, 1979) is  
348 calculated. The Cramer's  $V$  is considered as the more robust association test because of  
349 its possibility to assess large and complex contingency tables (Howell, 1997). The  
350 coefficient provides a standardized measure in the range [0-1]; the closer  $V \rightarrow 1$ , the  
351 stronger is the association between two PVs.
- 352 (iii) Exploration of the structure of the association between PV classes and the RV by a  
353 multiple correspondence analysis (MCA), and definition of the most significant classes  
354 of a PV to represent landslide occurrences.
- 355 (iv) Introduction of a neo-variable (nPv) with geomorphological meaning (van Westen et  
356 al., 2003) in the statistical model by combining PVs causing CI violations.

357 (v) Finally, the performance of each PV and nPV is assessed by introducing the variables  
358 iteratively in the statistical model. If the relative error does not decrease despite the  
359 addition of a PV or an nPV, the simulation is rejected; whereas, if the relative error  
360 decreases, the simulation is accepted.

361

### 362 3.2.3. Evaluation of performance of the indirect susceptibility maps

363 The performance of the indirect susceptibility maps was assessed for the total study area with  
364 the best combination of PVs and nPVs (Figs. 1 and 5). Both statistical and expert evaluations  
365 were performed successively.

366 First, the weights obtained for the classes of the best PVs and nPVs are applied to the total  
367 study area (Figs. 1 and 5) and the susceptibility classes were defined with the same thresholds  
368 in the cumulative curves. The degree of model fit was evaluated by analysing the  $\xi$  value for  
369 all the LTZs observed in the total study area. If  $\xi$  is low ( $<0.3$ ), the statistical model is  
370 considered as robust. Then, the confidence of PostP was evaluated by the Student-t test. This  
371 test uses the variance of PostP to create a normalized value to estimate the certainty of the  
372 calculation with the null hypothesis  $H_0$ : PostP = 0. The normalized value has to be equal or  
373 larger than 1.64 to have a certainty calculation of 95% (Bonham-Carter, 1994; Davis, 2002).

374 Second, the indirect susceptibility map was compared with the direct susceptibility map.  
375 Because the direct susceptibility map had been produced by the French Official Method of  
376 Landslide Risk Zoning (MATE/METL, 1999) independently of the landslide types, a unified  
377 indirect susceptibility map was produced by combining the indirect susceptibility maps  
378 obtained for the three landslide types. The four classes of the indirect susceptibility maps  
379 were merged, and for each cell, more weight was systematically given to the higher  
380 susceptibility class (Fig. 8). Confusion matrices were calculated and several statistical tests

381 were performed for the direct and unified indirect susceptibility maps (Tables 5 and 6). The  
382 Kappa ( $K$ ) coefficient was used to assess the improvement of the model predictions over  
383 chance (Table 6). A  $K$  value of 1 is equivalent to a perfect agreement between the model and  
384 the reference map.  $K$  values higher than 0.4 signify a good statistical agreement between  
385 maps (Fielding and Bell, 1997).

386

## 387 **4. Results**

### 388 *4.1. Best response variable*

389 The minimum number of cells representing the variability of the predisposing factors within  
390 the LTZs was identified from the 460 cells. The relation between the number of LTZs cells  
391 introduced in the model and  $\xi$  for each landslide type is presented in Fig. 7. A threshold  
392 comparable to 50% of the 460 cells was identified to stabilize  $\xi$  for the ‘sampling area’, and  
393 the simulations with RV-3 to RV-7 were performed with the 230 cells. Table 4 indicates that  
394 the simulations with RV-2 and RV-3 are not acceptable, confirming that using only one or a  
395 few cells around the centre of a LTZ mass underestimates PriorP and PostP. Table 4 also  
396 indicates the influence of LTZ sizes on the results, and highlights that the best results are  
397 obtained with the use of the cells representing the most frequent combination of PVs observed  
398 in LTZs (RV-7).

399

### 400 *4.2. Best predictive variables*

401 Statistical tests indicate CI violation between the PVs. As an example, the values of the  $\chi^2$ -test  
402 and the Cramer’s  $V$  coefficient for the translational slides are detailed in Table 7. The

403 Cramer's  $V$  coefficient indicates a low association between the variables except for SLO-CUR  
404 and SLO-SF. The correlation SLO-CUR is mainly related to the location of RV-7 cells on  
405 slopes between  $15^\circ$  and  $35^\circ$ , which cover more or less 50% of the 'sampling area' and present  
406 planar slopes. Therefore, the information contained in these two PVs is redundant and  
407 combining these variables has no geomorphological meaning. Consequently, the PV CUR  
408 was not introduced in the statistical model. In contrast, the combination of variables with a  
409 geomorphological meaning (for instance SLO and SF) was introduced.

410 The first four axes of the MCA (multiple correspondence analysis) explain 40.5%, 49.3% and  
411 46.0% of the total variance for the shallow translational slides, rotational slides and  
412 translational slides, respectively. Despite the low contribution of each axis ( $<20\%$ ) on the  
413 cumulated variance, some useful information is still highlighted by the MCA. For example,  
414 the axes F1, F2 and F3 of the translational slides confirm the relation between SLO and the  
415 surficial formations (SF and TSF). Thus, the MCA gives some indications on the possible  
416 combination of classes for each PV, and allows us to justify the definition of an nPV with  
417 both a geomorphological meaning and a low redundancy of information. Table 8 summarizes  
418 the results of the MCA for the three landslide types. Fig. 8 details the cumulative curves  
419 associated with each WOE simulations and the different thresholds to define the four  
420 susceptibility classes for each landslide type. Fig. 9 presents the susceptibility maps obtained  
421 for the shallow translational slides. Simple geomorphological information given by the nPV  
422 increases the performance of the models. For example, for the shallow translational slides, the  
423 best simulation carried out with the non-combined PVs (SLO, FS, LIT, and LAD) is  
424 characterized by a  $\xi$  value of 0.45 (Table 6), while the best simulation with the introduction of  
425 nPV-1 (which combines slope gradient classes and surficial formation types, Table 9) is  
426 characterized by a  $\xi$  value of 0.14 (Table 9). For the simulations performed in the 'sampling

427 area',  $\xi$  values are 0.18, 0.16, and 0.14 for the shallow translational slides, rotational slides,  
428 and translational slides, respectively (Table 9).

429

#### 430 4.3. Evaluation of indirect susceptibility maps

431 Fig. 10 presents the indirect susceptibility maps for each landslide type obtained by applying  
432 the PostP of the 'sampling area' to the total study area. The maps show a good agreement  
433 with the landslide inventory map and are characterized by  $\xi$  values of 0.22, 0.25 and 0.23 for  
434 the shallow translational slides, the rotational slides, and the translational slides, respectively  
435 (Table 10). The surfaces of high, moderate and low susceptibility are 4.9 km<sup>2</sup>, 1.6 km<sup>2</sup> and 1.6  
436 km<sup>2</sup> for the shallow translational slides, 12.3 km<sup>2</sup>, 5.1 km<sup>2</sup> and 6.3 km<sup>2</sup> for the translational  
437 slides, 3.8 km<sup>2</sup>, 2.2 km<sup>2</sup> and 3.2 km<sup>2</sup> for the rotational slides, and 12.3 km<sup>2</sup>, 5.1 km<sup>2</sup> and 6.3  
438 km<sup>2</sup> for the translational slides, respectively. The certainty test indicates a percentage of  
439 presence of the high susceptibility class in the confidence zone of 70.8%, 88.7% and 87.5%  
440 for the shallow translational slides, rotational slides, and translational slides, respectively.  
441 Consequently the high susceptibility classes simulated with the statistical models  
442 incorporating an nPV are relevant from a statistical viewpoint.

443 The unified indirect susceptibility map (Fig. 11) was then compared to the direct  
444 susceptibility map (Fig. 12). The former map identifies 17.7 km<sup>2</sup>, 5.8 km<sup>2</sup> and 6.9 km<sup>2</sup> of the  
445 high, medium and low susceptibility classes, respectively (Fig. 11). The confusion matrix  
446 (Table 11) indicates a good accuracy between the direct and indirect maps, especially for the  
447 high susceptibility class. Fig. 13 presents the observed differences between the two maps  
448 concerning the high susceptibility class.

449

450 **5. Discussion**

451 The proposed methodology to assess landslide susceptibility at 1:10 000 scale is based on a  
452 bivariate method calibrated on a 'sampling area' and validated on a larger area. To obtain a  
453 robust and reproducible procedure, simple and easy-to-obtain thematic data with a high cost-  
454 benefit ratio were used. The thematic maps introduced in the statistical model represent slope  
455 gradient, slope curvature, surficial formations, thickness of surficial formations, lithology,  
456 land use and streams. Our work indicates that introducing only simple PVs in the statistical  
457 model does not satisfactorily recognise landslide-prone areas in a complex environment.  
458 Therefore, the concept of nPV, the use of the main set of predisposing factors for one  
459 landslide type, was employed. In our case this set is essentially represented by the  
460 combination of the thematic classes of slope gradients and surficial deposits. An nPV is  
461 identified by analysing the structure of the relationships between the landslide types, slope  
462 gradients and surficial formations. The nPV significantly increases the performance of the  
463 three statistical models, as pointed out by the decrease of the  $\xi$  value from 0.45 to 0.14 for the  
464 shallow translational slides, 0.43 to 0.16 for the rotational slides, and 0.40 to 0.18 for the  
465 translational slides. Evaluation of the statistical model for the total study area shows good  
466 agreement among the indirect susceptibility map, the landslide inventory map, and the direct  
467 susceptibility map. However, to obtain a good agreement, several considerations have to be  
468 pointed out:

- 469 (i) Our indirect susceptibility maps represent better the high susceptibility class than the  
470 low to moderate susceptibility classes. Tables 10 and 11 confirm the good agreement of  
471 the indirect susceptibility map with the landslide inventory map and the direct  
472 susceptibility map for the high susceptibility class. The indirect susceptibility maps  
473 underestimate the surfaces of the low and moderate susceptibility classes with  $K$  values  
474 of 0.03 and 0.08, respectively. These disagreements are explained by the methodology

475 used to produce the direct and indirect susceptibility maps. On the one hand, rules  
476 relying on expert judgments can take into account (i) some subtle changes in specific  
477 areas which modify the degree of susceptibility, and (ii) the possibility of spatial  
478 evolution of landslides. On the other hand, statistical models were developed in our  
479 study to recognize areas favourable for active LTZs. The calculation processes of such  
480 models are based on binary evidences and are optimized to recognize areas with  
481 identical environmental characteristics, and the procedure of calibration/validation of the  
482 models is dependent on the thresholds observed on the simulated cumulative curves  
483 (Begueria, 2006; van den Eeckhaut et al., 2006). If this classification/validation  
484 procedure is employed, some potentially landslide-prone areas may be overestimated or  
485 underestimated (Begueria, 2006), and consequently the low and moderate susceptibility  
486 classes are not very well identified on the cumulative curve.

487 (ii) Our indirect susceptibility maps may not take some portion of terrain into account. For  
488 instance, in our study, the portions of terrain with slope gradients lower than  $15^\circ$  are  
489 always considered with a low or null susceptibility, although some of such areas are  
490 prone to landsliding. This discrepancy may be explained by the analysis used to select  
491 the best RV (RV-7) which mathematically increases the weights of the PV combination  
492 corresponding to the LTZs, and by the underestimation of PostP for these slope  
493 gradients because only a few LTZs are located on these slopes.

494 (iii) On a more general viewpoint, the 'sampling area' has to be selected carefully. Indeed, if  
495 the 'sampling area' is not sufficiently representative of the environmental conditions of  
496 the total study area, calculations of PriorP and PostP are biased. If the study area is  
497 sufficiently large, a sensitivity analysis on several 'sampling areas' with different sizes  
498 and shapes is recommended in order to select the more appropriate area which  
499 represents the total study area (Greco et al., 2007). In our case, the study area has a

500 complex topography with two distinct parts and several landslide types. Therefore, the  
501 selection of the 'sampling area' was based on geomorphological knowledge of the site.

502 (iv) Statistical models are very sensitive to the type and number of landslide cells. A  
503 conceptual model has therefore been created for each landslide type, because each type  
504 is controlled by a specific combination of predisposing factors. Furthermore, the quality  
505 of the indirect susceptibility maps depends on the selection of relevant cells representing  
506 the variability of the environmental factors (Greco et al., 2007).

507 (v) Statistical models are also very sensitive to the thematic data of environmental factors,  
508 and to their potential conditional dependence. Regarding CI violation, the results of the  
509  $\chi^2$ -test and the value of the  $V$  coefficient have to be interpreted with caution, because a  
510 few cells can severely bias the results (Dumolard et al., 2003). These tests are just  
511 informative and they cannot be used in rigorous terms (Pistocchi et al., 2002).  
512 Therefore, instead of not incorporating the cells posing some problems or decreasing the  
513 total number of RV cells, the proposed procedure intends to combine some classes of  
514 the PVs which are conditionally dependent. Indeed, decreasing the number of RV cells  
515 could modify the stability of the model as demonstrated previously. A robust procedure  
516 to follow is to combine an expert judgment with the  $\chi^2$ -test and the  $V$  coefficient in a  
517 multiple correspondence analysis, in order to identify the classes of PVs violating CI  
518 and select the classes of PVs to be combined with an nPV with a geomorphological  
519 meaning. As mentioned by van Westen et al. (2003, 2006), expert judgment is very  
520 important in the conception of the statistical model to guide thematic maps towards  
521 geomorphological landslide evidences. Regarding the minimum set of thematic maps,  
522 the different statistical tests used in our study stress the difficulty to map landslide  
523 susceptibility at 1:10,000 scale using only a few variables. Other data sources such as a  
524 more detailed soil thickness map or detailed structural maps (fault map and tectonic

525 map) should be used in order to obtain more accurate results. Nevertheless, at this scale  
526 of work and for a large and complex environment, these variables are extremely difficult  
527 to measure because of their high spatial variability. Therefore, they have been often  
528 neglected in susceptibility assessment.

529 The proposed procedure follows the guidelines suggested by van Westen et al. (2003) and  
530 Guzzetti et al. (2006) for the validation of indirect susceptibility maps. Guzzetti et al. (2006)  
531 proposed a set of criteria for ranking and comparing the quality of landslide susceptibility  
532 assessments, i.e., the quality of the input data and the use of different statistical tests. In terms  
533 of these criteria, the susceptibility maps obtained with the procedure used in this study have  
534 the highest quality (level 7).

## 535 **6. Conclusion**

536 This study has demonstrated the necessity of using specific and adapted procedures for  
537 indirect landslide susceptibility assessment by bivariate methods, especially at 1:10,000 scale,  
538 for complex environments with some uncertainty in collected landslide characteristics. The  
539 proposed procedure, based on a reduced number of thematic data and a 'sampling area',  
540 consists of four steps. First, the best response variable RV (e.g. landslide inventory) to be  
541 introduced in the statistical model is defined. This variable may vary according to the  
542 landslide type and the environmental characteristics of the study area. Second, the best PVs  
543 (e.g. terrain predisposing factors) to be used in the statistical model are identified by  
544 minimizing conditional dependence on the basis of statistical tests. The structure of the  
545 statistical relation between RV and PV is studied through multiple correspondence analyses to  
546 identify the class of PVs influencing the location of landslides. Based on the results, neo-  
547 predictive variables (nPVs) with geomorphological meanings are proposed, and introduced in  
548 the statistical models. Third, the performance and confidence associated with the simulations

549 are evaluated by statistical tests and expert knowledge. Fourth, more appropriate thematic  
550 data and weights identified on the 'sampling area' are applied to the total study area. The  
551 results are compared to a direct landslide susceptibility map through a confusion matrix.

552 The procedure was applied successfully to the north-facing hillslope of the Barcelonnette  
553 Basin. The indirect and direct susceptibility maps are quite similar for the high susceptibility  
554 class with a high classification rate and a good Kappa ( $K$ ) coefficient.

555 This study has demonstrated that the use of a 'sampling area' correctly representing the  
556 geomorphology of a larger area, combined with the use of neo-predictive variables, is  
557 sufficient to calibrate a bivariate statistical model for landslide susceptibility assessment. This  
558 study reinforces the use of bivariate statistical models based on both expert knowledge and  
559 objective calculations for landslide susceptibility assessment, assuming the use of specific  
560 statistical tests if only a few landslide data are available. The proposed procedure has to be  
561 tested in other types of environment in order to verify its spatial robustness.

562

### 563 **Acknowledgements**

564 This research was financially supported by the European Union through the research  
565 programme ALARM (Assessment of Landslide Risk and Mitigation in Mountain Areas),  
566 contract EVG1-2001-00018, 2002-2004, Coordinator: S. Silvano (CNR-IRPI, Padova).

567

### 568 **References**

569 Agterberg, F.P., Bonham-Carter, G.F., Cheng, Q., Wright, D.F., 1993. Weights of evidence modeling and weighted logistic  
570 regression for mineral potential mapping. In: Davis, J.C., Herzfeld, U.C. (Eds.), Computer in Geology, 25 Years of  
571 Progress. Oxford University Press, Oxford, pp. 13-32.

- 572 Agterberg, F.P., Cheng, Q., 2002. Conditional independence test for weights of evidence modeling. *Natural Resources*  
573 *Research* 11, 249-255.
- 574 Aleotti, P., Chowdhury, R., 1999. Landslide hazard assessment: summary review and new perspectives. *Bulletin of*  
575 *Engineering Geology and the Environment* 58, 21-44.
- 576 Atkinson, P.M., Massari, R., 1998. Generalised linear modelling of susceptibility to landsliding in the central Apennines,  
577 Italy. *Computers and Geosciences* 24, 373-385.
- 578 Ardizzone, F., Cardinali, M., Carrara, A., Guzzetti, F., Reichenbach, P., 2002. Uncertainty and errors in landslide mapping  
579 and landslide hazard assessment. *Natural Hazard and Earth System Science* 2, 3-14.
- 580 Begueria, S., Lorente, A., 1999. Landslide Hazard Mapping by Multivariate Statistics: a Comparison of Methods and Case  
581 Study in the Spanish Pyrenees. The Damocles Project Work, Contract N° EVG1-CT 1999-00007. Technical Report. 20 pp.
- 582 Bégueria, S., 2006. Validation and evaluation of predictive models in hazard assessment and risk management. *Natural*  
583 *Hazards* 17, 315-329.
- 584 Bonham-Carter, G.F., 1994. *Geographic Information System for Geoscientists: Modelling with GIS*. Pergamon Press,  
585 Oxford. 398 pp.
- 586 Bonham-Carter, G.F., Agterberg, F.P., Wright, D.F., 1989. Weights of evidence modelling: a new approach to mapping  
587 mineral potential. In: Agterberg, F.P., Bonham-Carter, G.F. (Eds.), *Statistical Applications in Earth Sciences*. Geological  
588 Survey of Canada, Ottawa, pp. 171-183.
- 589 Bonham-Carter, G.F., Agterberg, F.P., Wright, D.F., 1990. Statistical pattern integration for mineral exploration. In: Gaal, G.,  
590 Merriam D.F. (Eds.), *Computer Applications in Resource Estimation: Prediction and Assessment for Metals and*  
591 *Petroleum*. Pergamon Press, Oxford, pp. 1-21.
- 592 Brabb, E.E., 1984. Innovative approaches to landslide hazard mapping. *Proceedings of Fourth International Symposium on*  
593 *Landslides*, Toronto, pp. 307-324.
- 594 BRGM, 1974. Carte et notice géologique de Barcelonnette au 1:50 000ème, XXXV-39. Bureau des Recherches Géologiques  
595 et Minières. Orléans.
- 596 Carrara, A., Cardinali, M., Guzzetti, F., Reichenbach, P., 1995. GIS technology in mapping landslide hazard. In: Carrara, A.,  
597 Guzzetti, F. (Eds.), *Geographical Information Systems in Assessing Natural Hazards*. Kluwer, Dordrecht, pp. 135-176.
- 598 Chàcon, J., Irigaray, C., Fernández, T., El Hamdouni, R., 2006. Engineering geology maps: landslides and geographical  
599 information systems. *Bulletin of Engineering Geology and the Environment* 65, 341-411.
- 600 Chung, C.F., 2006. likelihood ratio functions for modeling the conditional probability of occurrence of future landslides for  
601 risk assessment. *Computers and Geosciences*, 32, 1052-1068.

- 602 Chung, C. F., Fabbri, A. G., 2003. Validation of spatial prediction models for landslide hazard mapping. *Natural Hazards*, 30,  
603 451–472.
- 604 Chung, C.F., Fabbri, A.G., van Westen, C.J., 1995. Multivariate regression analysis for landslide hazard zonation. In:  
605 Carrara, A., Guzzetti, F. (Eds.), *Geographical Information Systems in Assessing Natural Hazards*. Kluwer, Dordrecht, pp.  
606 107-133.
- 607 Clerici, A., Perego, S., Tellini, C., Vescovi, P., 2002. A procedure for landslide susceptibility zonation by the conditional  
608 analysis method. *Geomorphology* 48, 349-364.
- 609 Crozier, M.J., Glade, T., 2005. Landslide hazard and risk: Issues, Concepts and Approach. In: Glade, T., Anderson, M.,  
610 Crozier, M.J. (Eds.), *Landslide Hazard and Risk*. Wiley, Chichester, pp. 1-40.
- 611 Dai, F.C., Lee, C.F., Ngai, Y.Y., 2002. Landslide risk assessment and management overview. *Engineering Geology* 64, 65-  
612 87.
- 613 Davis J.C., 2002. *Statistics and Data Analysis in Geology*, Third Edition. John Wiley & Sons, New York, 638 pp.
- 614 Dikau, R., Brunsten, D., Schrott, L., Ibsen M-L., 1996. *Landslides Recognition, Identification, Movement and Causes*. John  
615 Wiley & Sons, New York, 251 pp.
- 616 Dumolard, P., Dubus, N., Charleux, L., 2003. *Les statistiques en géographie*. Ed. Belin. Paris, 239 pp.
- 617 Fell, R., 1994. Landslide risk assessment and acceptable risk. *Canadian Geotechnical Journal* 31, 261-272.
- 618 Fielding, A.H., Bell, J.F., 1997. A review of methods for the assessment of prediction errors in conservation presence/  
619 absence models. *Environmental Conservation* 24, 38-49.
- 620 Flage ollet, J-C., Maquaire, O., Martin, B., Weber, D., 1999. Landslides and climatic conditions in the Barcelonnette and Vars  
621 basins Southern French Alps, France. *Geomorphology* 30, 65-78.
- 622 Glade, T., Crozier, M.J., 2005. A review of scale dependency in landslide hazard and risk analysis. In: Glade, T., Anderson,  
623 M., Crozier, M.J. (Eds.), *Landslide Hazard and Risk*. John Wiley and Sons, Chichester, pp. 75-138.
- 624 Greco, R., Sorriso-Valvo, M., Catalano, E., 2007. Logistic Regression analysis in the evaluation of mass movements  
625 susceptibility: the Aspromonte case study, Calabria, Italy. *Engineering Geology* 89, 47-66.
- 626 Guzzetti, F., Carrara, A., Cardinali, M., Reichenbach, P., 1999. Landslide hazard evaluation: a review of current techniques  
627 and their application in a multi-scale study, central Italy. *Geomorphology* 31, 181–216.
- 628 Guzzetti, F., Reichenbach, P., Ardizzone, F., Cardinali, M., Galli, M., 2006. Estimating the quality of landslide susceptibility  
629 models. *Geomorphology* 81, 166-184.

- 630 Hansen, A., 1984. Landslide hazard analysis. In: Brunsdon, D., Prior, D.B. (Eds.), Slope Instability. John Wiley & Sons, New  
631 York, pp. 532-602.
- 632 Howell, D.C., 1997. Statistical Methods for Psychology. Fourth Edition. ITP, De Boeck University, 768 pp.
- 633 Kojima, H., Chung, C.F., Van Westen, C.J., 2000. Strategy on landslide type analysis based on expert knowledge and the  
634 quantitative prediction model. International Archives of Photogrammetry & Remote Sensing 33, 701-708.
- 635 Kemp, L.D., Bonham-Carter, G.F., Raines, G.L., Looney, C.G., 2001. Arc-SDM: Arcview extension for spatial data  
636 modelling using weights of evidence, logistic regression, fuzzy logic and neural network analysis,  
637 <http://ntserv.gis.nrcan.gc.ca/sdm/>
- 638 Kendall, M., Stuart, A., 1979. The Advanced Theory of Statistics: Inference and Relationship. Griffin, London, 748 pp.
- 639 Leroi, E., 2005. Global rockfalls risk management process in 'La Désirade' Island (French West Indies). Landslides 2, 358-  
640 365.
- 641 Malet, J-P., Van Asch, Th.W.J., van Beek, R., Maquaire, O., 2005. Forecasting the behaviour of complex landslides with a  
642 spatially distributed hydrological model. Natural Hazards and Earth System Sciences 5, 71-85.
- 643 Maquaire, O., Malet, J.P., Remaître, A., Locat, J., Klotz, S., Guillon, J., 2003. Instability conditions of marly hillslopes:  
644 towards landsliding or gullyng? The case of the Barcelonnette basin, South-East France. Engineering Geology 70, 109-  
645 130.
- 646 MATE/MATL, 1999. Plan de Prévention des Risques (PPR): Risques de Mouvements de terrain, Ministère de  
647 l'Aménagement du Territoire et de l'Environnement (MATE), Ministère de l'Équipement des Transports et du Logement  
648 (METL). La Documentation Française, Paris. 74 pp.
- 649 Pistocchi A., Luzi, L., Napolitano, P., 2002. The use of predictive modelling techniques for optimal exploitation of spatial  
650 databases: a case study in landslide hazard mapping with expert system-like methods. Environmental Geology 41, 765-  
651 775.
- 652 Remondo, J., González-Diez, A., Diaz de Terán, J.R., Cendrero, A., 2003. Landslides susceptibility models utilising spatial  
653 data analysis techniques. A case study from the lower Deba Valley, Guipúzcoa (Spain). Natural Hazards 30, 267-279.
- 654 Soeters R., Van Westen C.J., 1996. Slope instability, recognition, analysis, and zonation. In: Turner, A.K., Schuster, R.L.  
655 (Eds.), Landslides Investigation and Mitigation, Transportation Research Board, Special Report 247. National Research  
656 Council, Washington, pp. 129-177.
- 657 Soriso Valvo, M., 2002. Landslides; from inventory to risk. In Rybář, J., Stemberk, J., Wagner, P. (Eds.), Landslides,  
658 Proceedings of the International European Conference on Landslides. Balkema, Rotterdam, pp. 79-93.

- 659 Spiegelhater, D., Kill-Jones, R.P., 1984. Statistical and knowledge approaches to clinical decision-support systems, with an  
660 application in gastroenterology. *Journal of the Royal Statistical Society* 147, 35-77.
- 661 Sterlacchini S., Maseti M., Poli, S. 2004. Spatial integration of thematic data for predictive landslide mapping: a case study  
662 from Oltrepo Pavese area, Italy. In: Lacerda W.A., Ehrlich M., Fountoura, S.A.B., Sayão, A.S.F. (Eds.), *Landslides*  
663 *Evaluation and Stabilization*. Balkema, Rotterdam, pp. 109-116.
- 664 Süzen, M.L., Doyuran, V., 2004. Data driven bivariate landslide susceptibility assessment using geographical information  
665 systems: method and application to Asarsuyu catchment, Turkey. *Engineering Geology* 71, 303-321.
- 666 Thiart, C., Bonham-Carter, G.F., Agterberg, F.P., 2003. Conditional independence in weights of evidence: application of an  
667 improved test. IAMG, International Association for Mathematical Geology, September 7th-12th, 2003, Portsmouth,  
668 United-Kingdom.
- 669 Thiery, Y., Puissant, A., Malet, J-P., Remaitre, A., Beck, E., Sterlacchini, S., Maquaire, O., 2003. Towards the construction  
670 of a spatial database to manage landslides with GIS in mountainous environment. In: *Proceedings of AGILE 2003: The*  
671 *Science behind the Infrastructure*, 6<sup>th</sup> AGILE Conference on Geographic Information Science. 24th-26th, April 2003,  
672 Lyon, France, pp. 37-44.
- 673 Thiery Y., Sterlacchini S., Malet J-P., Puissant A., Maquaire O., 2004. Strategy to reduce subjectivity in landslide  
674 susceptibility zonation by GIS in complex mountainous environments. In: Toppen, F., Prastacos, P. (Eds.), *Proceedings of*  
675 *AGILE 2004: 7th AGILE Conference on Geographic Information Science*. 29th April – 1st May 2004, Heraklion, Greece,  
676 pp. 623-634.
- 677 Thiery, Y., Malet, J-P., Sterlacchini, S., Puissant, A., Maquaire, O., 2005 *Analyse spatiale de la susceptibilité des versants*  
678 *aux mouvements de terrain, comparaison de deux approches spatialisées par SIG*. *Revue internationale de*  
679 *géomatique/European journal of GIS and spatial analysis* 15, 227-245.
- 680 Van den Eeckhaut, M., Vanwalleghem, T., Poesen, J., Govers, G., Verstraeten G., Vandekerckhove, L., 2006. Prediction of  
681 landslide susceptibility using rare events logistic regression: a case-study in the Flemish Ardennes (Belgium).  
682 *Geomorphology* 76, 392-410.
- 683 Van Westen, C.J., 1993. *Application of Geographic Information Systems to Landslide Hazard Zonation*. ITC Publication,  
684 vol. 15. International Institute for Aerospace and Earth Resources Survey, Enschede, 245 pp.
- 685 Van Westen, C.J., 2004. Geo-Information tools for landslide risk assessment: an overview of recent developments. In  
686 Lacerda W.A., Ehrlich M., Fountoura, S.A.B., Sayão, A.S.F. (Eds.), *Landslides Evaluation and Stabilization*. Balkema,  
687 Rotterdam, pp. 39-56.
- 688 Van Westen C.J., Rengers N., Soeters R., 2003. Use of geomorphological information in indirect landslide susceptibility  
689 assessment. *Natural Hazards* 30, 399-419.

- 690 Van Westen C.J., Van Asch, Th.W.J., Soeters, R., 2006. Landslide hazard and risk zonation: why is it still so difficult?  
691 Bulletin of Engineering Geology and the Environment 65, 167-184.
- 692 Varnes, D.J., 1984, Landslide Hazard Zonation, a Review of Principles and Practice. IAEG Commission on Landslides,  
693 UNESCO, Paris. 63 pp.
- 694 Wills C.J., McCrinck, T.P., 2002. Comparing landslide inventories: the map depends on the method. Environmental and  
695 Engineering Geoscience 8, 279-293.
- 696 Yin, K.L., Yan, T.Z., 1988. Statistical prediction model for slope instability of metamorphosed rocks. In: Bonnard, C. (Ed.),  
697 Landslides, Proceedings of Fifth International Symposium in Landslides. Balkema, Rotterdam, pp. 1269-1272.

Table 1. Morphometric characteristics of active landslides inventoried with a high mapping confidence index (MCI).  $\mu$  is geometric average;  $\sigma$  is standard deviation.

| Landslide type              | Number | Depth (m) |          | Width (m) |          | Length (m) |          | Slope of LTZ (°) |          | Landslide size (m <sup>2</sup> ) |          | Size of LTZ (m <sup>2</sup> ) |          |
|-----------------------------|--------|-----------|----------|-----------|----------|------------|----------|------------------|----------|----------------------------------|----------|-------------------------------|----------|
|                             |        | $\mu$     | $\sigma$ | $\mu$     | $\sigma$ | $\mu$      | $\sigma$ | $\mu$            | $\sigma$ | $\mu$                            | $\sigma$ | $\mu$                         | $\sigma$ |
| Shallow translational slide | 50     | 2         | 0.6      | 60        | 25       | 77         | 70       | 31               | 9        | 2766                             | 2389     | 866                           | 714      |
| Rotational slide            | 54     | 6         | 3        | 140       | 136      | 118        | 114      | 21               | 9        | 12527                            | 12971    | 4601                          | 3947     |
| Translational slide         | 88     | 6.5       | 4.5      | 78        | 70       | 217        | 168      | 21               | 6        | 14874                            | 19002    | 4400                          | 4100     |

Table 2. Thematic data used in the statistical model.

| Themes              | Map                           | Source of information and methods used   |
|---------------------|-------------------------------|--|
| Landslide inventory | Landslide inventory map (LAI) | API (air-photo interpretation), field survey, analysis of available documents                                    |
| Relief              | Slope gradient map (SLO)      | DTM elaborated by digitization and interpolation of elevation lines extracted from topographical maps (1:10,000) |
|                     | Slope curvature map (CUR)     |  |
| Geology             | Lithological map (LIT)        | Analysis of geological map, field survey   |
|                     | Surficial formation map (SF)  | Analysis of geological and geomorphological maps, field survey   |
|                     | Thickness map (TSF)           | Field survey   |
|                     | Bedding map (BED)             | Analysis of geological map, field survey   |
| Hydrology           | Distance to stream map (HYD)  | API, analysis of topographical maps  |
| Landuse             | Landuse map (LAD)             | SIA (satellite imagery analysis), API, field survey  |

Table 3. Expert rules and associated environmental conditions used to define the direct susceptibility map. SLO: slope gradient; LAD: land use; CUR: slope curvature.

| Susceptibility class           | Expert rule   | Environmental conditions  |
|--------------------------------|---|---|
| S0:<br>no susceptibility       | Environmental conditions favourable to slope stability. No possibility of landslide developments for the next one hundred years.  | SLO: 0-10°<br>LAD: arable land, permanent crop  |
| S1:<br>low susceptibility      | Environmental conditions are slightly favourable to slope instability. Low possibility of landslide developments for the next one hundred years. Future human and socio-economic developments of the area are possible and subject to specific attention. | SLO: 10-20°<br>LAD: pasture, grassland<br>CUR: moderate presence of topographic irregularities  |
| S2:<br>moderate susceptibility | Environmental conditions are moderately favourable to slope instability. Moderate possibilities of landslide developments for the next one hundred years. Mitigation works are essential for future human and socio-economic developments of the area.    | SLO: 20-30°<br>LAD: pasture, grassland, forests lowly maintained<br>CUR: high presence of topographic irregularities, hummocky topography |
| S3:<br>high susceptibility     | Environmental conditions are very favourable to slope instability. High possibility of landslide developments for the next one hundred years. Future human and socio-economic developments of the area are impossible.                                    | SLO: > 30°<br>LAD: landuse highly deteriorated, bare soils, forests not maintained<br>CUR: very hummocky topography                       |

Table 4. Characteristics of the response variable (RV) introduced in the statistical model to identify the most relevant spatial locations of cells to represent the variability of predisposing factors within LTZs, and relative error associated with the simulations. The simulations were performed with the predictive variables (PVs) SLO, SF, LIT and LAND (Table 2). STS: shallow translational slides; RS: rotational slides; TS: translational slides.

| Response variable (RV) | Characteristics of the response variable  | Relative error $\xi$ (-) |      |      |
|------------------------|---|--------------------------|------|------|
|                        |   | STS                      | RS   | TS   |
| RV-1                   | Use of all (460) cells of the landslide triggering zones (LTZs)   | 0.50                     | 0.54 | 0.45 |
| RV-2                   | Use of the centre of mass of each LTZ (e.g. one cell per LTZ)   | 0.76                     | 0.73 | 0.74 |
| RV-3                   | Use of the total number of cells in a radius of 10 m around RV-2 (e.g. 230 cells)   | 0.57                     | 0.60 | 0.49 |
| RV-4                   | Use of the total number of cells of small LTZs (mean size: TS: 215 m <sup>2</sup> ; RS: 260 m <sup>2</sup> ; STS: 60 m <sup>2</sup> )       | 0.64                     | 0.69 | 0.69 |
| RV-5                   | Use of the total number of cells of medium-size LTZs (mean size: TS: 400 m <sup>2</sup> ; RS: 450 m <sup>2</sup> ; STS: 65 m <sup>2</sup> ) | 0.58                     | 0.62 | 0.52 |
| RV-6                   | Use of the total number of cells of large LTZs (mean size: TS: 650 m <sup>2</sup> ; RS: 640 m <sup>2</sup> ; STS: 190 m <sup>2</sup> )      | 0.53                     | 0.54 | 0.46 |
| RV-7                   | Use of the cells representing the most frequent combination of PVs observed in each LTZ (e.g. 230 cells)                                    | 0.45                     | 0.43 | 0.40 |

Table 5. Confusion matrix. a: true positives; b: false positives; c: false negatives; d: true negatives.

|           |                | Observed       |                |
|-----------|----------------|----------------|----------------|
|           |                | X <sub>1</sub> | X <sub>0</sub> |
| Predicted | X <sub>1</sub> | A              | b              |
|           | X <sub>0</sub> | C              | d              |

Table 6. Statistics derived from the confusion matrix. N: number of cells in the study area. a: true positives; b: false positives; c: false negatives; d: true negatives.

|                             |   |   |
|-----------------------------|---|---|
| Correct classification rate | $(a + d) / N$   | Proportion of correctly classified observations   |
| Misclassification rate      | $(b + c) / N$   | Proportion of incorrectly classified observations |
| Sensitivity                 | $a / (a + c)$   | Proportion of positive cases correctly predicted  |
| Specificity                 | $d / (b + d)$   | Proportion of negative cases correctly predicted  |
| Kappa (K) coefficient       | $[(a + d) - (((a + c)(a + b) + (b + d)(c + d)) / N)] / [N - (((a + c)(a + b) + (b + d)(c + d)) / N)]$ | Proportion of specific agreement                  |

Table 7. Example of association measures between RV-7 and PVs for the translational slides. The PVs CUR, HYD and BED are not introduced in the model because there is no causal relation between the occurrence of the translational slides and these PVs. The bold font indicates the PV used to build an nPV.  $\chi^2$ -test: from left to right, calculated  $\chi^2$ , theoretical  $\chi^2$ , and degree of freedom. The grey-coloured box represents the conditional dependence between PVs and the null hypothesis  $H_0$  rejected for a level of significance  $\alpha = 0.05$ . Cramer's  $V$  coefficient: the bold font indicates moderate to high association between the variables.

| PV         |          | LIT          | SF           | TSF             | LAD            | CUR           |
|------------|----------|--------------|--------------|-----------------|----------------|---------------|
| <b>SLO</b> | $\chi^2$ | 2.6 12.5 (6) | 33.1 21 (12) | 104.3 28.8 (18) | 75.5 36.4 (24) | 81.6 21 (12)  |
|            | $V$      | 0.11         | <b>0.42</b>  | 0.26            | 0.29           | <b>0.41</b>   |
| LIT        | $\chi^2$ | -            | 0.2 5.9 (2)  | 5.7 7.8 (3)     | 0.2 9.5 (4)    | 1.2 5.9 (2)   |
|            | $V$      | -            | 0            | 0.15            | 0.03           | 0.07          |
| SF         | $\chi^2$ | -            | -            | 9.6 12.5 (6)    | 35.3 15.5 (8)  | 7.2 9.4 (6)   |
|            | $V$      | -            | -            | 0.14            | 0.27           | 0.12          |
| TSF        | $\chi^2$ | -            | -            | -               | 31.8 21 (12)   | 55.7 12.6 (6) |
|            | $V$      | -            | -            | -               | 0.2            | 0.38          |
| LAD        | $\chi^2$ | -            | -            | -               | -              | 24.5 9.5 (4)  |
|            | $V$      | -            | -            | -               | -              | 0.23          |

Table 8. Contribution of PVs on the explained variance of the axes F1 to F4 for three landslide types. The most contributive PVs for each axis are indicated in grey and are used to define nPVs. The classes chosen to build nPVs are detailed in the last column.

|                                     | SLO   | LIT  | SF   | TSF  | LAD  | CUR  | HYD  | BED  | Explained variance (%) | Structure of nPVs  |
|-------------------------------------|-------|------|------|------|------|------|------|------|------------------------|--|
| <i>Shallow translational slides</i> |       |      |      |      |      |      |      |      |                        |  |
| F1                                  | 25.6  | 18.6 | 19.1 | 3.2  | 15.3 | 0.1  | 0.1  | 18.2 | 13.1                   | nPV-1: SLO (15-25°, 25-35°, 35-45°, 45-55°) + SF (colluvium, scree, moraine deposit) |
| F2                                  | 10.3  | 6.9  | 5.9  | 21.5 | 25.9 | 3.6  | 0.2  | 25.6 | 22.7                   |  |
| F3                                  | 18.4  | 16.5 | 6.9  | 25.0 | 16.4 | 2.0  | 10.4 | 4.5  | 32                     |  |
| F4                                  | 21.64 | 3.3  | 10.0 | 28.1 | 28.5 | 7.4  | 0.7  | 0.3  | 40.5                   |  |
| <i>Rotational slides</i>            |       |      |      |      |      |      |      |      |                        |  |
| F1                                  | 33.1  | 17.2 | 24.9 | 3.0  | 21.0 | 0.6  | 0.05 | -    | 16.4                   | nPV-3: SLO (10-20°, 20-30°, 30-40°) + SF (all classes)                               |
| F2                                  | 24.9  | 3.8  | 0.8  | 34.2 | 7.8  | 19.7 | 2.4  | -    | 28.4                   |  |
| F3                                  | 19.8  | 17.0 | 6.7  | 29.7 | 9.2  | 11.2 | 6.4  | -    | 39.8                   |  |
| F4                                  | 40.9  | 0.9  | 4.5  | 22.5 | 20.6 | 0.7  | 10.0 | -    | 49.3                   |  |
| <i>Translational slides</i>         |       |      |      |      |      |      |      |      |                        |  |
| F1                                  | 37.1  | 0.4  | 25.6 | 21.1 | 15.7 | -    | -    | -    | 12.9                   | nPV-3: SLO (5-15°, 15-25°, 25-35°, 35-45°) + SF (moraine deposit)                    |
| F2                                  | 36.8  | 3.1  | 6.3  | 29.9 | 20.6 | -    | -    | -    | 25.3                   |  |
| F3                                  | 39.9  | 0.1  | 12.2 | 33.8 | 13.7 | -    | -    | -    | 36.1                   | nPV-4: SLO (25-35°, 35-45°) + SF (colluvium or weathered marl)                       |
| F4                                  | 24.3  | 2.4  | 25.7 | 16.7 | 30.8 | -    | -    | -    | 46.0                   |  |

Table 9. Relative error  $\xi$  and CI results for the best combination of PVs and nPVs

| Landslide type                     | Combination                   | $\xi$ | $\chi^2$ -test | V-coefficient |
|------------------------------------|-------------------------------|-------|----------------|---------------|
| Shallow translational slides (STS) | nPV-1 + LAD                   | 0.40  | Yes            | Low           |
|                                    | nPV-1 + LAD + HYD             | 0.35  | Yes            | Low           |
|                                    | nPV-1 + LAD + HYD + CUR       | 0.21  | Yes            | Low           |
|                                    | nPV-1 + LAD + HYD + CUR + BED | 0.14  | Yes            | Low           |
| Rotational slides (RS)             | nPV-2 + LAD                   | 0.21  | Yes            | Low           |
|                                    | nPV-2 + LAD + HYD             | 0.18  | Yes            | Low           |
|                                    | nPV-2 + LAD + HYD + CUR       | 0.16  | Yes            | Low           |
| Translational slides (TS)          | nPV-3 + LIT                   | 0.35  | Yes            | Low           |
|                                    | nPV-3 + LIT + LAD             | 0.18  | Yes            | Low           |

Table 10. Relative error  $\xi$  of the best simulations for the 'sampling area' and the total study area. Results are indicated for the LTZ and the total area of landslide (L). Simulations are computed with RV-7.

|                          | STS<br>(nPV-1 + LAD + HYD + CUR + BED) |      | RS<br>(nPV-2 + LAD + HYD + CUR) |      | TS<br>(nPV-3 + LIT + LAD) |      |
|--------------------------|--|------|---------------------------------|------|---------------------------|------|
|                          | LTZ                                    | L    | LTZ                             | L    | LTZ                       | L    |
|                          | $\xi$ : 'sampling area'                | 0.14 | 0.09                            | 0.16 | 0.34                      | 0.18 |
| $\xi$ : total study area | 0.22                                   | 0.26 | 0.21                            | 0.33 | 0.23                      | 0.47 |

Table 11. Statistical accuracy tests between the indirect and direct susceptibility maps. ccr is the correct classification rate; mcr is misclassification rate.

|                | Susceptibility class |      |          |      |        |
|----------------|----------------------|------|----------|------|--------|
|                | Null                 | Low  | Moderate | High | Global |
| ccr            | 0.73                 | 0.81 | 0.85     | 0.91 | 0.61   |
| mcr            | 0.27                 | 0.19 | 0.15     | 0.09 | 0.39   |
| sensitivity    | 0.87                 | 0.18 | 0.08     | 0.80 | 0.61   |
| spec ificity   | 0.39                 | 0.89 | 0.95     | 0.93 | 0.89   |
| Kappa <i>K</i> | 0.36                 | 0.08 | 0.03     | 0.43 | 0.41   |

Fig. 1. Shaded relief map of the north-facing hillslope of the Barcelonnette Basin and distribution of landslides.

Fig. 2. Landuse map of the north-facing hillslope of the Barcelonnette Basin.

Fig. 3. Simplified geological map (A) and observed landslide types in the Barcelonnette Basin: (B) shallow translational slide in the Abriès Torrent; (C) rotational slide in the Poche Torrent; and (D) translational slide in the Bois Noir catchment.

Fig. 4. Characteristics of the active landslides observed in the Barcelonnette Basin.

Fig. 5. Strategy for susceptibility assessment with the bivariate WOE model at 1:10,000 scale.

Fig. 6. Distribution of landslides and environmental characteristics of the 'sampling area'. (A) inventory of active landslides; (B) slope gradient map; (C) surficial formations map; (D) lithological map; (E) landuse map; (F) thickness of surficial formations map; (G) irregularities of terrain map; (H) outcrop and type of dip map.

Fig. 7. Relative error  $\xi$  of the simulations for several quantities of RV cells introduced in the statistical model.

Fig. 8. Cumulative curves of the best simulation obtained in the 'sampling area'. (A) translational slides; (B) rotational slides; (C) shallow translational slides. The susceptibility classes are defined on the basis of the thresholds observed in the cumulative curves of total probabilities. The number of cells in the highest susceptibility class is compared to the distribution of LTZs (relative error  $\xi$ ).

Fig. 9. Example of WOE simulations for shallow translational slides performed without (A) and with (B) the introduction of an nPV: Statistical simulations with the PVs SLO + SF + LIT + LAD and with the PVs nPV-1 + LAD + CUR + BED, respectively.

Fig. 10. Indirect susceptibility map for the landslide types observed on the north-facing hillslope of the Barcelonnette Basin. (A) shallow translational slides; (B) rotational slides; (C) translational slides.

Fig. 11. Direct susceptibility map produced with the French Official Method of Landslide Risk Zoning.

Fig. 12. Final indirect susceptibility map produced by combining the three indirect landslide susceptibility maps.

Fig. 13. Differences between the direct and final indirect susceptibility maps (example of the high susceptibility class).

Figure 1  
[Click here to download high resolution image](#)

hal-00276804, version 1 - 2 May 2008

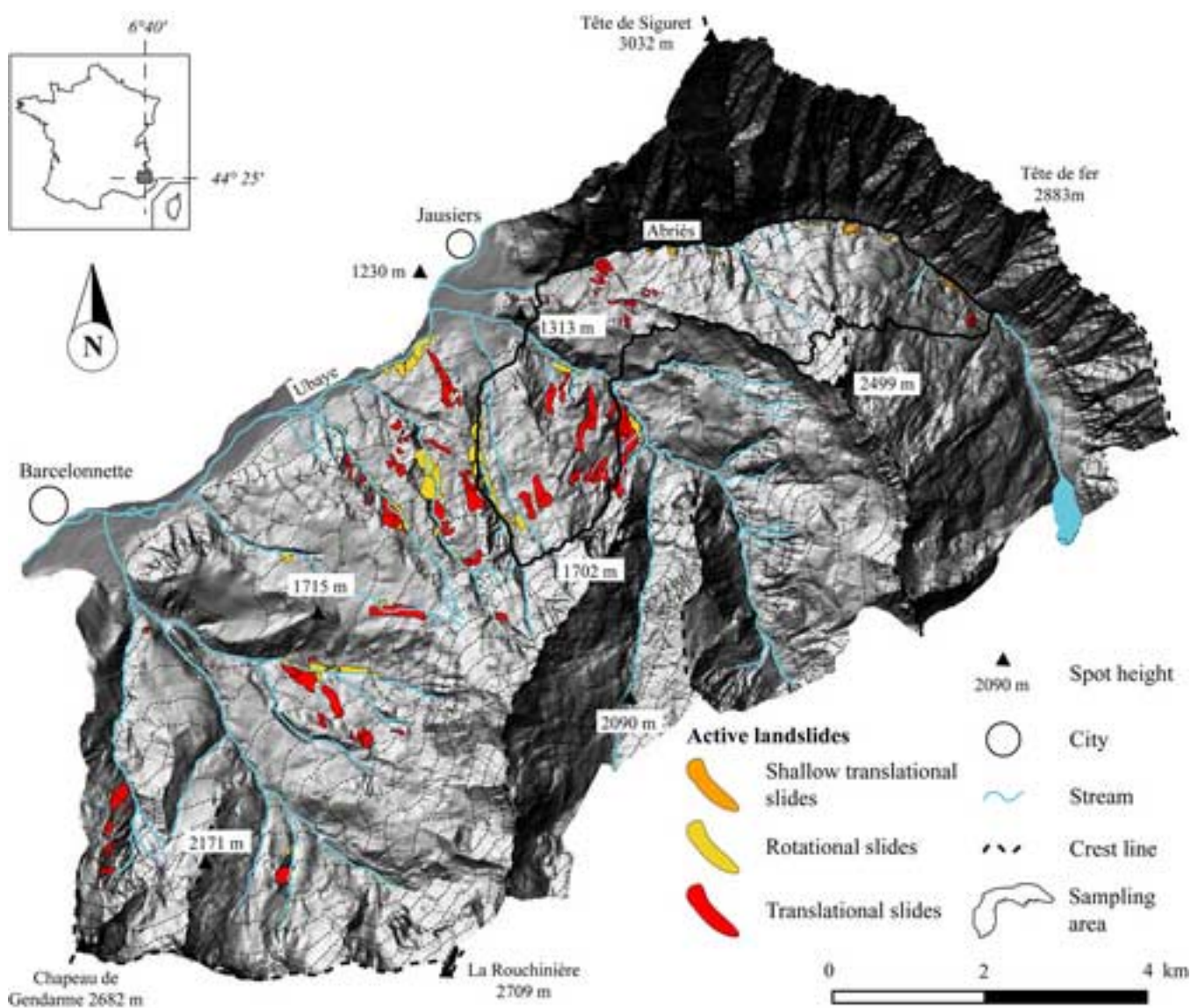


Figure 2  
[Click here to download high resolution image](#)

hal-00276804, version 1 - 2 May 2008

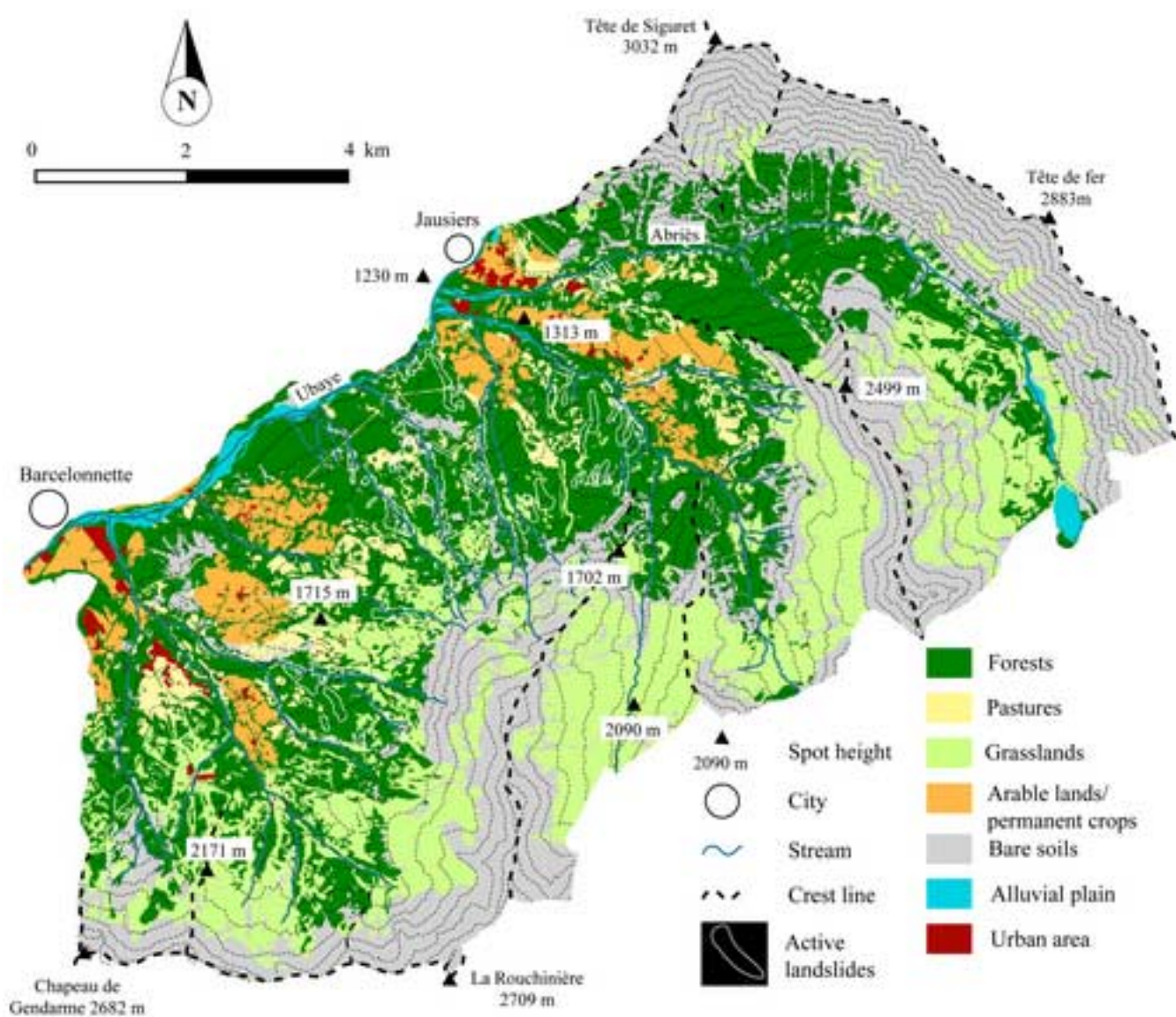


Figure 3  
[Click here to download high resolution image](#)

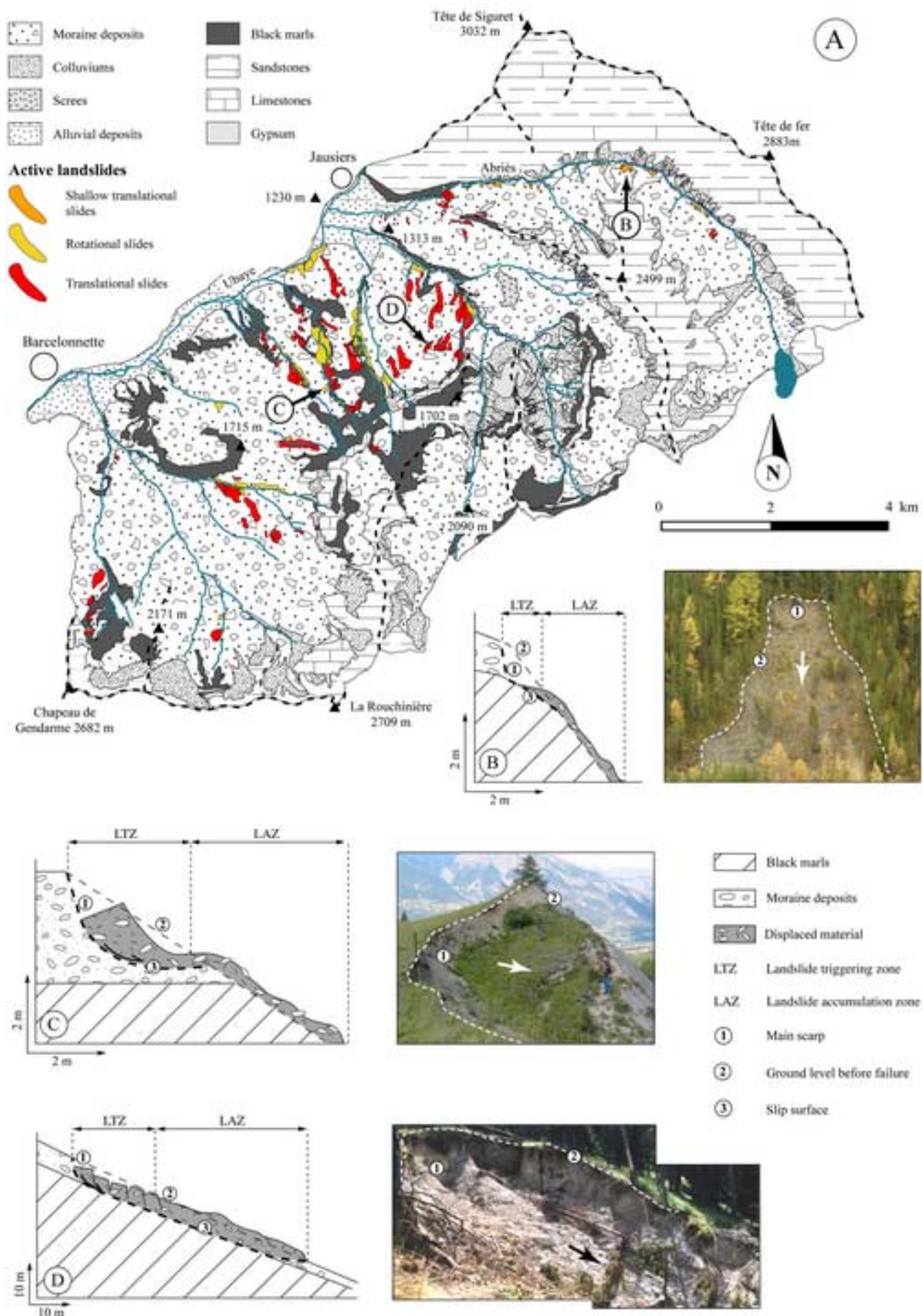


Figure 4  
[Click here to download high resolution image](#)

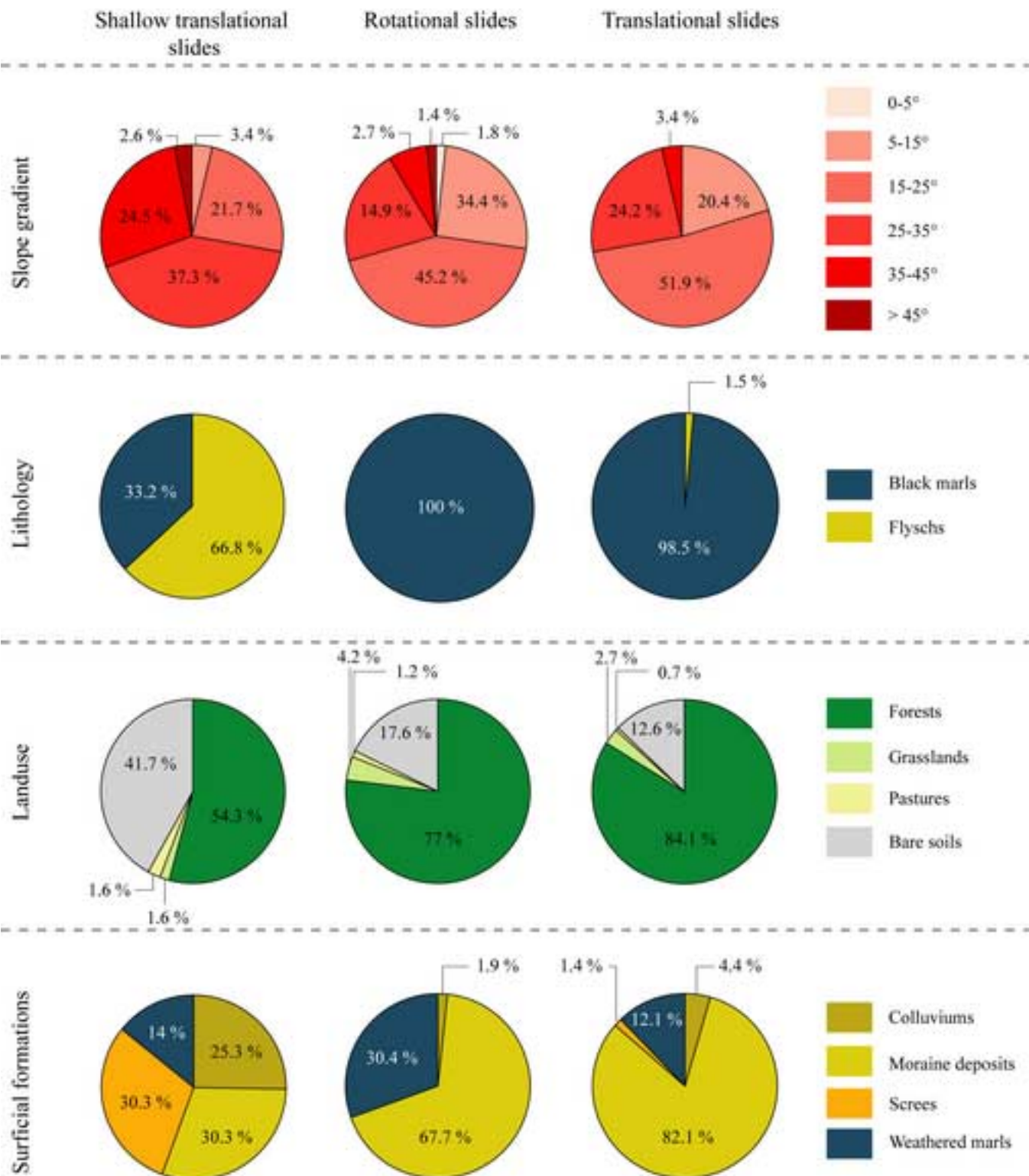


Figure 5  
[Click here to download high resolution image](#)

hal-00276804, version 1 - 2 May 2008

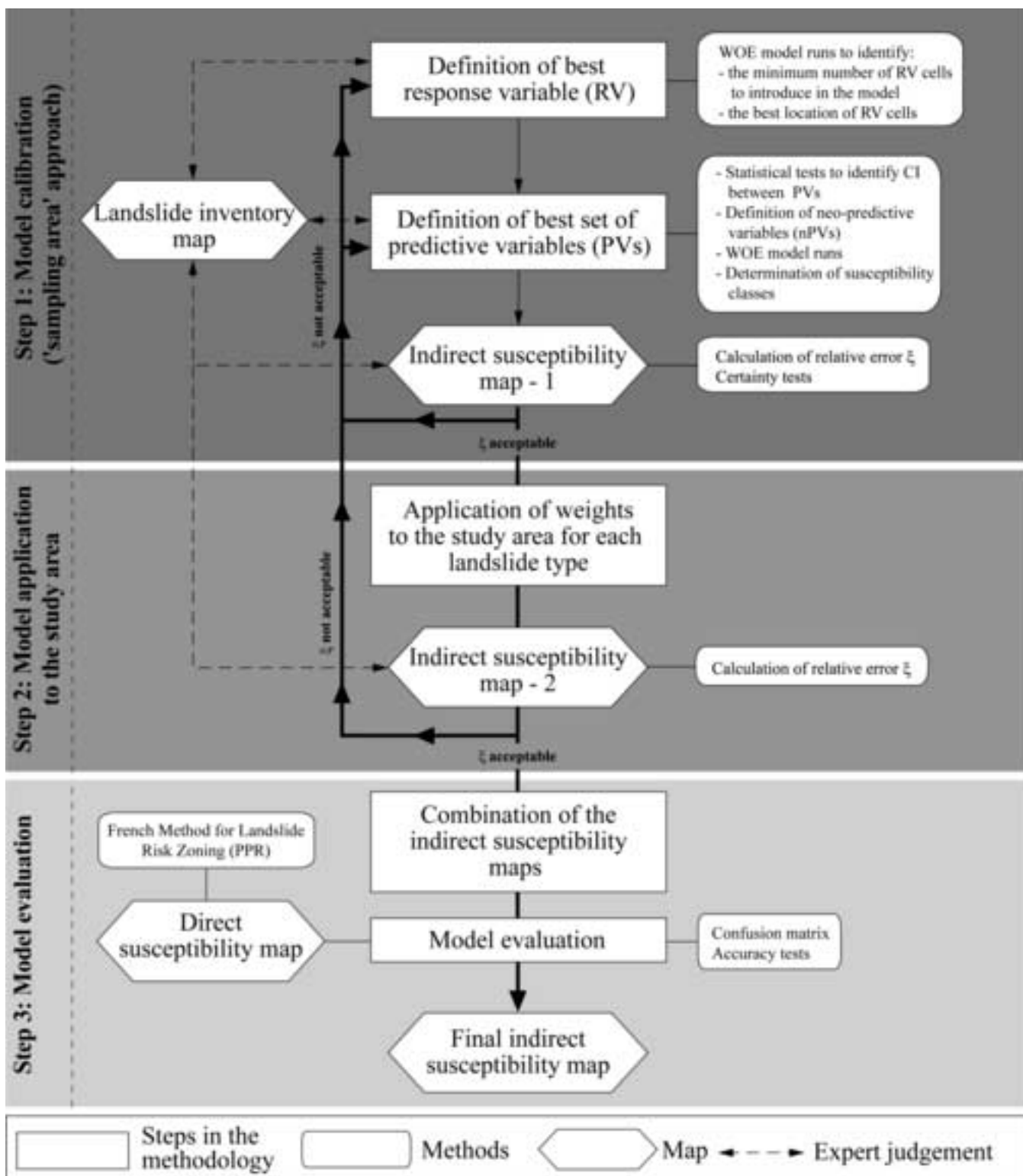


Figure 6  
[Click here to download high resolution image](#)

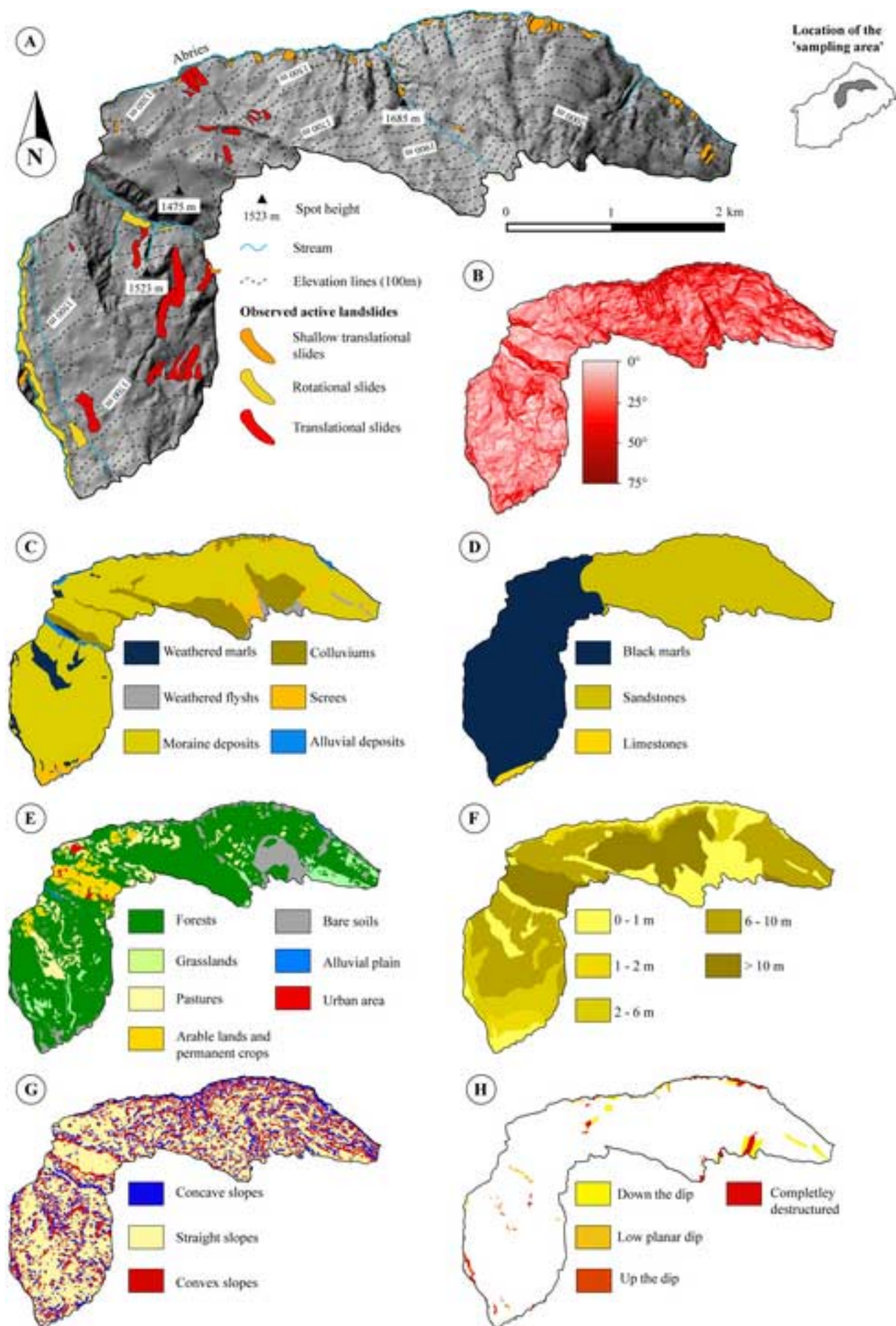
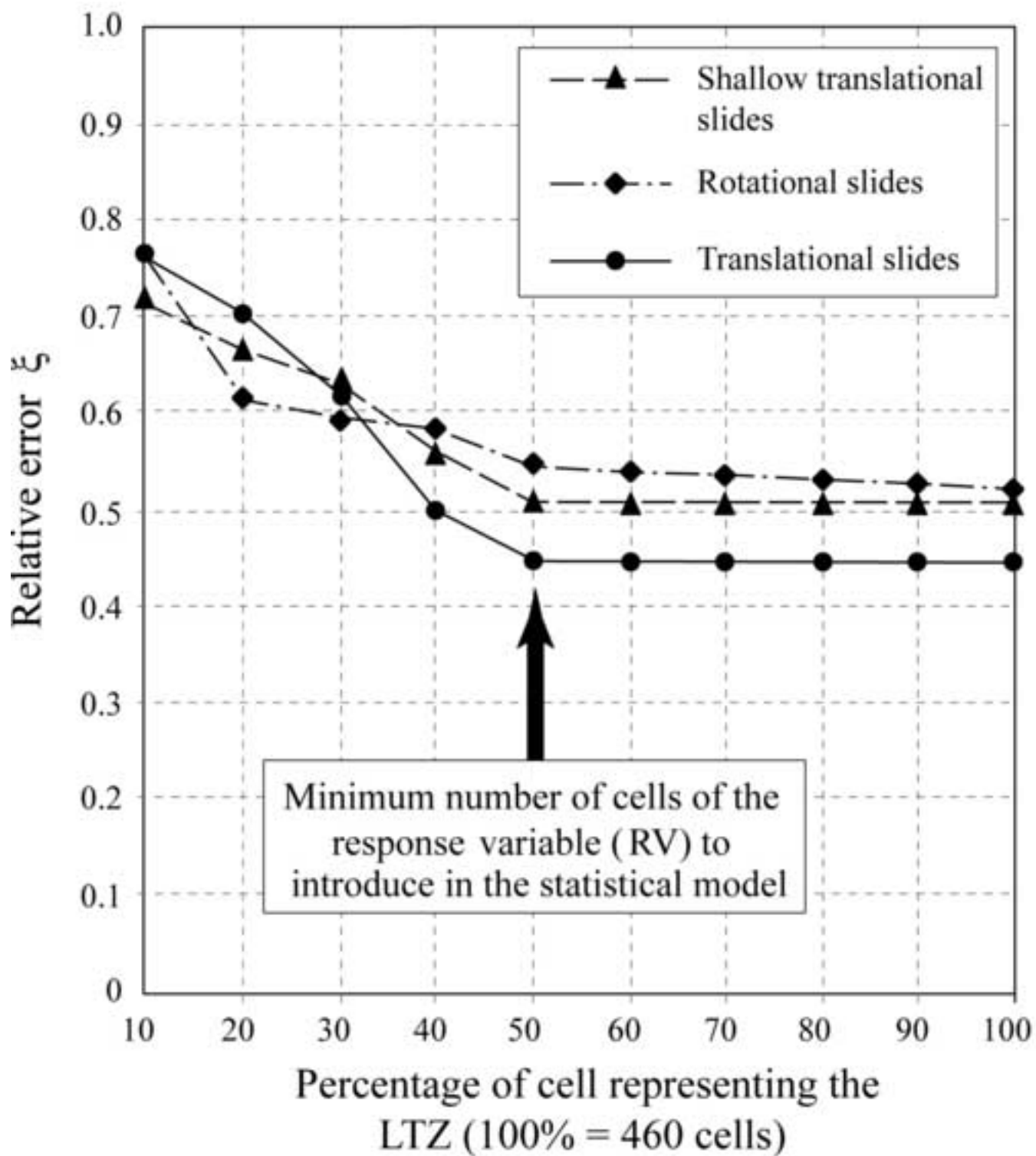
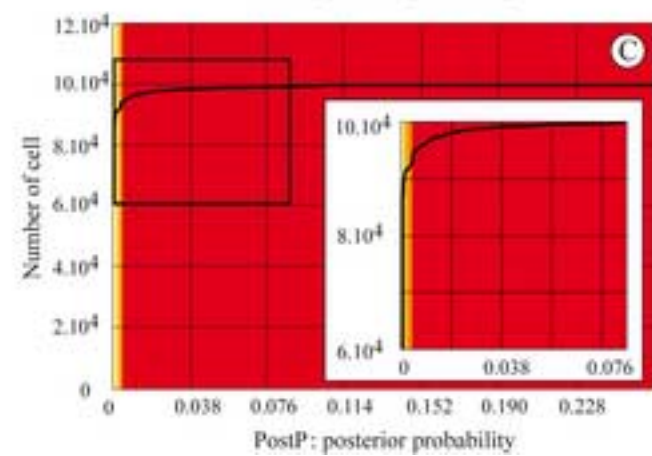
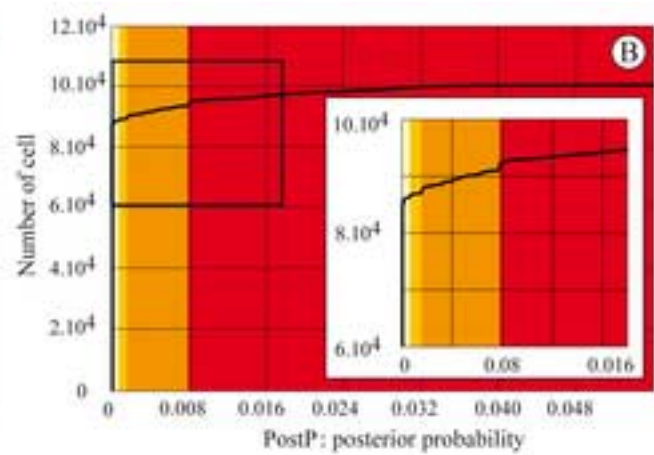
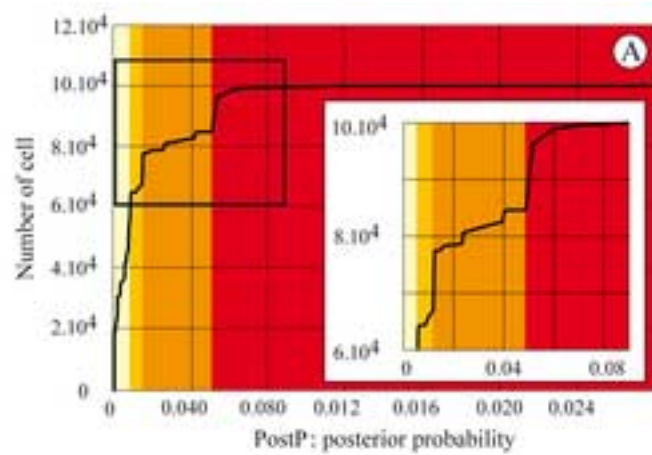


Figure 7  
[Click here to download high resolution image](#)



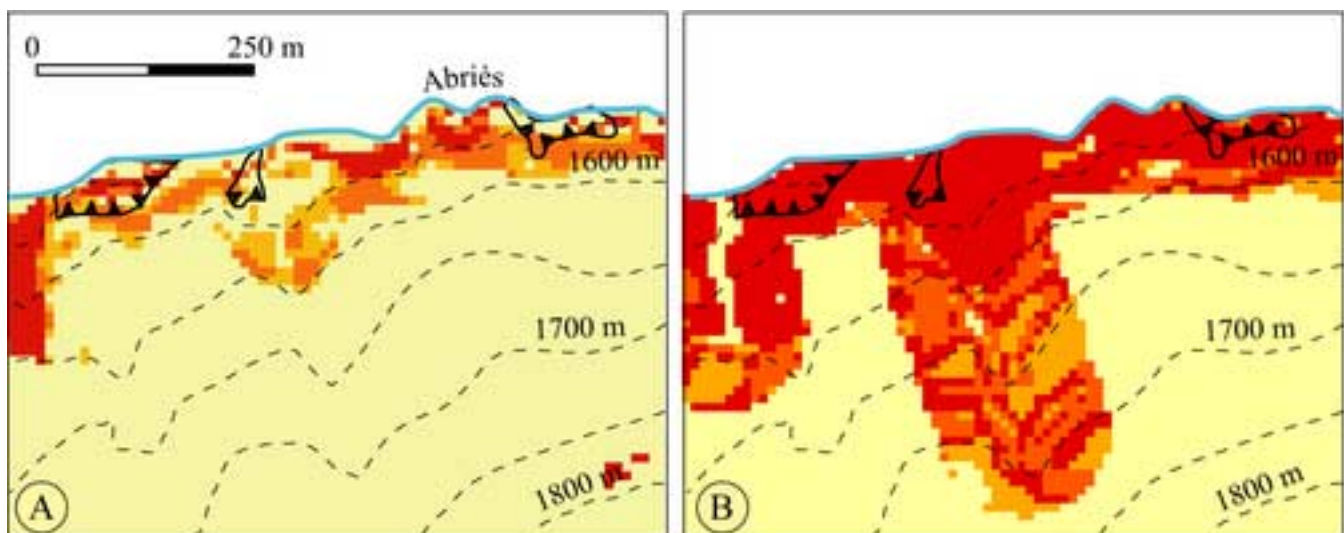
**Susceptibility class**

- Null
- Low
- Moderate
- High

Figure 9

[Click here to download high resolution image](#)

hal-00276804, version 1 - 2 May 2008



- Stream
- Elevation lines (50m)
- Shallow translational slides

**Susceptibility class**

- Null
- Low
- Moderate
- High

Figure 10  
[Click here to download high resolution image](#)

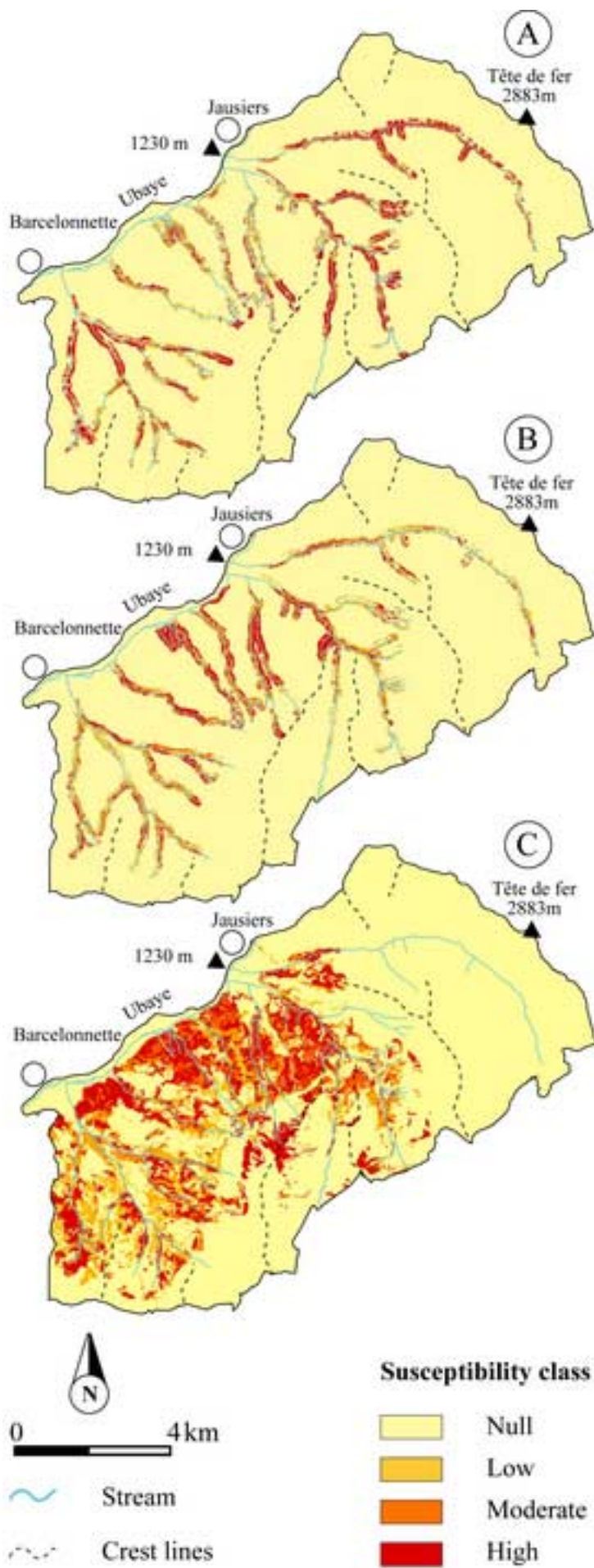


Figure 11  
[Click here to download high resolution image](#)

hal-00276804, version 1 - 2 May 2008

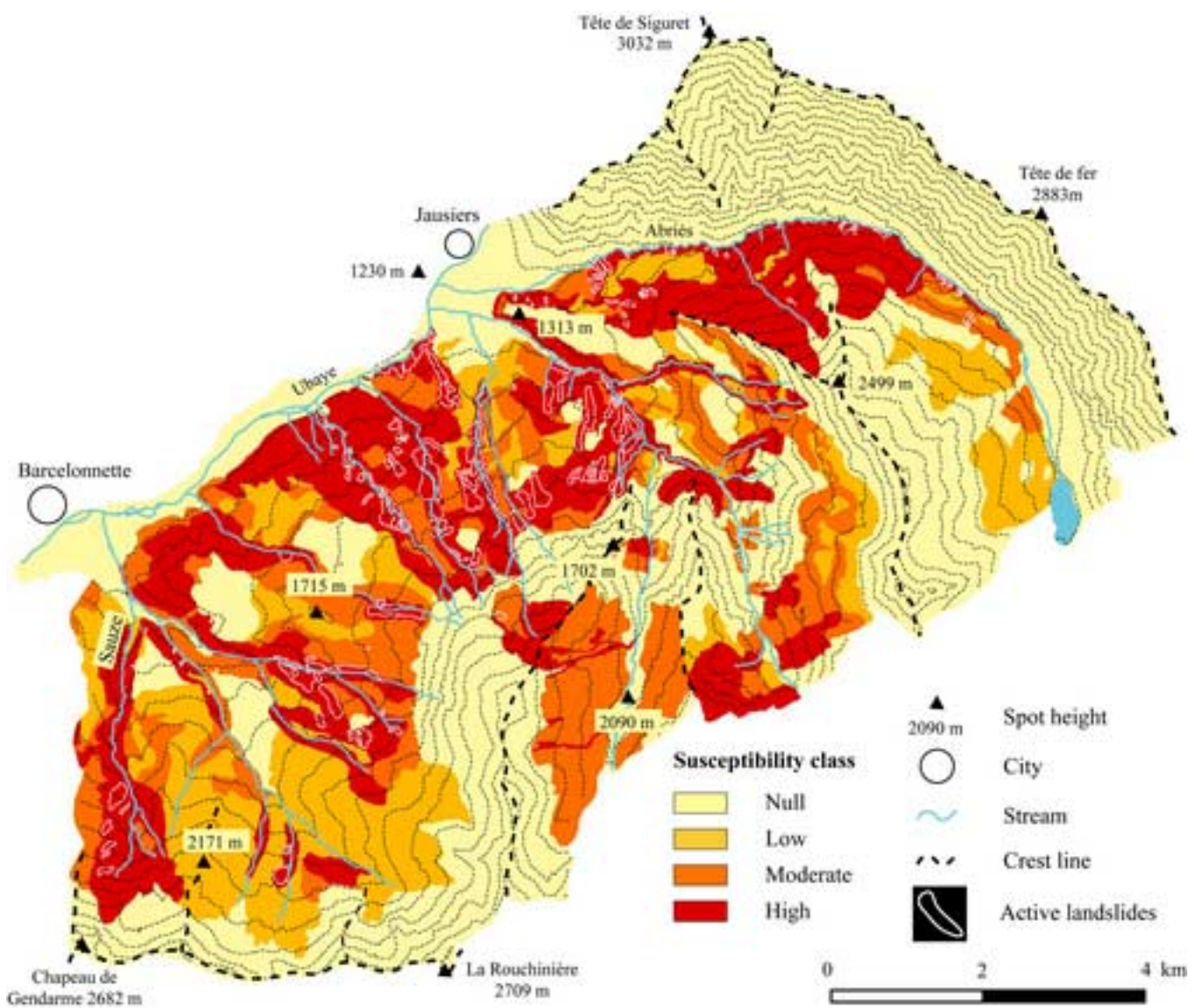


Figure 12  
[Click here to download high resolution image](#)

hal-00276804, version 1 - 2 May 2008

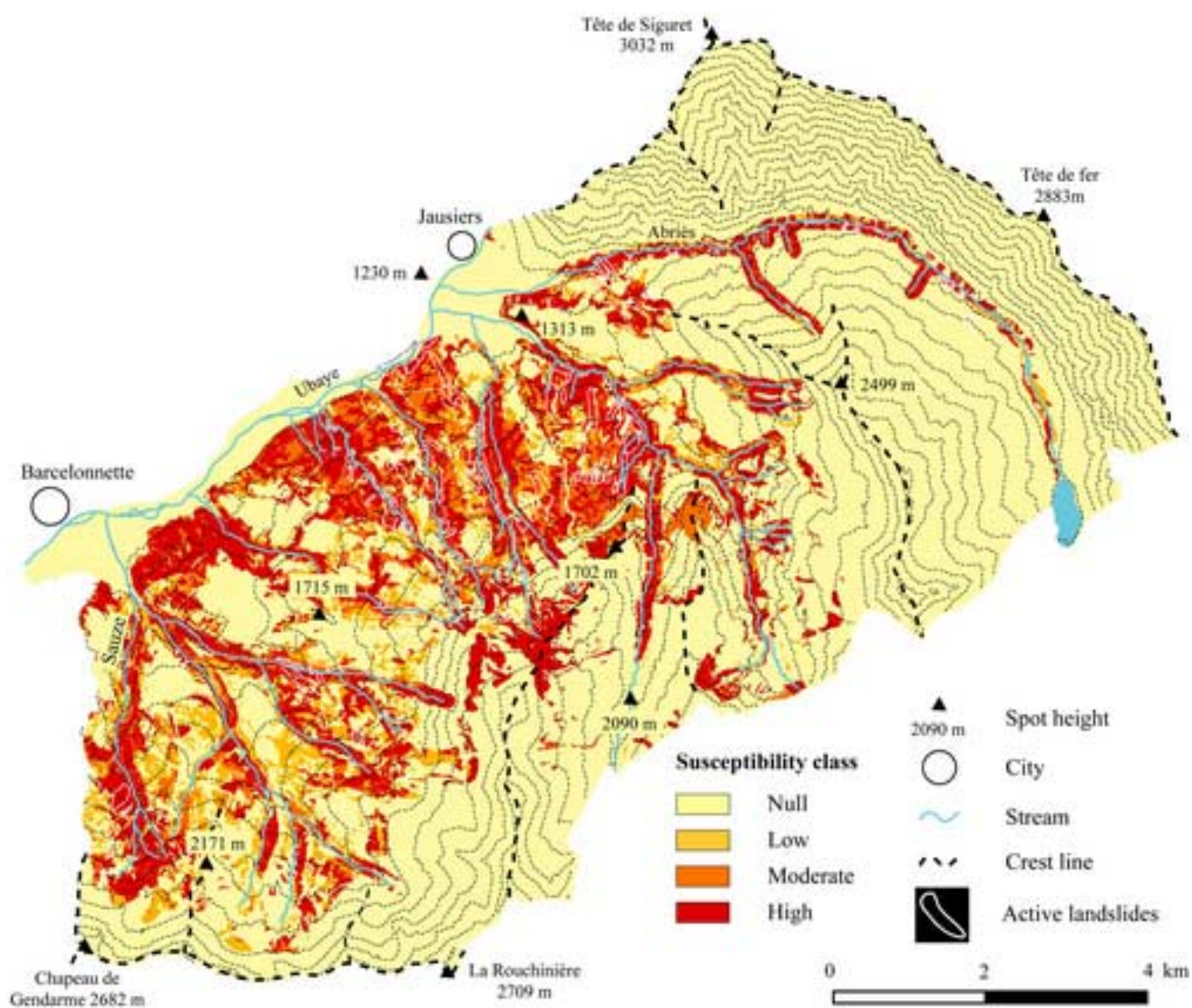


Figure 13  
[Click here to download high resolution image](#)

hal-00276804, version 1 - 2 May 2008

